

## **A history of ENSO events since A.D. 1525: implications for future climate change**

**Joëlle L. Gergis · Anthony M. Fowler**

Received: 19 December 2006 / Accepted: 12 May 2008 / Published online: 3 October 2008  
© Springer Science + Business Media B.V. 2008

**Abstract** Reconstructions of past climate are important for providing a historical context for evaluating the nature of 20th century climate change. Here, a number of percentile-based palaeoclimate reconstructions were used to isolate signals of both phases of El Niño–Southern Oscillation (ENSO). A total of 92 (82) El Niño (La Niña) events were reconstructed since A.D. 1525. Significantly, we introduce the most comprehensive La Niña event record compiled to date. This annual record of ENSO events can now be used for independent verification of climate model simulations, reconstructions of ENSO indices and as a chronological control for archaeologists/social scientists interested in human responses to past climate events. Although extreme ENSO events are seen throughout the 478-year ENSO reconstruction, approximately 43% of extreme and 28% of all protracted ENSO events (i.e. both El Niño and La Niña phase) occur in the 20th century. The post-1940 period alone accounts for 30% of extreme ENSO years observed since A.D. 1525. These results suggest that ENSO may operate differently under natural (pre-industrial) and anthropogenic background states. As evidence of stresses on water supply, agriculture and natural ecosystems caused by climate change strengthens, studies into how ENSO will operate under global warming should be a global research priority.

---

J. L. Gergis (✉)  
School of Earth Sciences, University of Melbourne, VIC, 3010 Melbourne, Australia  
e-mail: jgergis@gmail.com

A. M. Fowler  
School of Geography and Environmental Science, University of Auckland,  
Private Bag, 92019 Auckland, New Zealand

## 1 Introduction

Generated in the tropical Pacific, El Niño–Southern Oscillation (ENSO) events create a far-reaching system of climate anomalies that operate on a range of time scales important to society (Dunbar and Cole 1999). ENSO influences extreme weather events such as drought, flooding, bushfires and tropical cyclone activity across vast areas of the Earth, adversely affecting hundreds of millions of people in agriculturally important areas of Australasia, Africa and the Americas (Bouma et al. 1997; Dunbar and Cole 1999; Caviedes 2001; Chen et al. 2007). Despite being the dominant source of inter-annual climate variability, many characteristics of long-term changes in the frequency, duration and magnitude of ENSO events remain unknown (Crowley 2000; Grove and Chappell 2000).

ENSO is a coupled cycle in the atmosphere–oceanic system (Bjerknes 1966, 1969). It is an irregular phenomenon that alternates between its two phases, El Niño and La Niña, approximately every 2–7 years (Allan et al. 1996; Markgraf and Diaz 2000). ENSO is a periodic reorganisation of Sea Surface Temperature (SST) and atmospheric circulation in the tropical Pacific that results in vast redistributions of major rainfall-producing systems (Rasmusson and Carpenter 1983; Allan 2000). Generally, El Niño (La Niña) events cause a warming (cooling) in tropical Pacific and Indian Oceans that suppresses (enhances) rainfall in western (eastern) Pacific regions (Allan et al. 1996). A ‘typical’ ENSO event tends to last for 18–24 months with peaks in amplitude mostly occurring in the austral summer (December–February) (Rasmusson and Carpenter 1983; Allan 2000).

Although ENSO is phase-locked to the annual cycle episodes are known to differ in terms of their relative strengths, seasons of onset, maturity, overall duration, and the spatial extent of maximum SST anomalies in the tropical Pacific (Rasmusson and Carpenter 1982; Trenberth and Stepaniak 2001; Lyon and Barnston 2005). Rainfall, SST and wind field anomalies associated with ENSO events differ considerably from event to event, as ‘centres-of-action’ shift (Allan et al. 1996; Fedorov and Philander 2000). Since any major redistribution of equatorial rainfall regimes are communicated into extra-tropical regions via ‘teleconnections’, ENSO dominates climate variability in many parts of the tropics, sub-tropics and some mid-latitude regions (Allan et al. 1996; Kumar and Hoerling 1997).

The late 20th century contained a number of extreme and prolonged ENSO episodes (Trenberth and Hoar 1996), including the two most intense El Niños (1982–1983 and 1997–1998) and La Niñas (1988–1989, 1973–1974). Since the mid-1970s, ENSO changed in character, displaying a tendency towards a dominance of El Niño rather than the La Niña phase (Allan 2000; Fedorov and Philander 2000). This abrupt climate swing in tropical Pacific circulation corresponded to changes in the Inter-decadal Pacific Oscillation (Trenberth and Hoar 1996; Zhang et al. 1997, 1998; Salinger et al. 2001; Trenberth and Stepaniak 2001) and has been a catalyst for further research on the nature, structure and evolution of ENSO on decadal-century timescales.

The long-term context of apparently anomalous ENSO behaviour witnessed in recent decades has received limited attention (Crowley 2000; Folland et al. 2001; Mann 2003). It is widely recognised that instrumental time series (less than 150 years) are too short to assess whether 20th century ENSO behaviour is atypical (Trenberth and Hoar 1996, 1997; Allan and D’Arrigo 1999; Fedorov and Philander 2000; Gergis

and Fowler 2005; Mendelssohn et al. 2005; Solow 2006). Consequently, multi-century palaeoclimate reconstructions derived from long proxy records, such as annually resolved tree-ring, coral, ice-core and documentary records provide a long-term context for assessing the significance of the apparently anomalous ENSO variability of the recent past (Jones and Mann 2004). A detailed review of these approaches are provided by Gergis et al. (2006).

Ideally, exactly dated, climatically sensitive proxies from the equatorial Pacific ‘centres-of-action’ of ENSO would be used to reconstruct the core characteristics of ENSO, and all remaining annual resolution proxies could then be used to map the spatial anomaly patterns of tropical and extra-tropical teleconnections associated with each reconstructed ENSO event (Stahle et al. 1998). Unfortunately, this ideal approach of reconstructing tropical ENSO variability and associated extra-tropical anomalies is hardly even possible for the 20th century due to the limited spatial coverage of instrumental data and the restricted network of precisely dated, annually resolved proxies currently available (Stahle et al. 1998).

The non-stationary nature of ENSO makes any reconstruction using proxy archives problematic (Gergis et al. 2006). The recent 2004–2005 El Niño was an instructive example of a decoupled ENSO event. SST anomalies exceeded 0.5°C in the western-central Pacific (Niño 4, Niño 3.4 and Niño 3 regions), while warming greater than 1°C did not expand eastward of 140°W, resulting in near zero anomalies along the ‘classical’ El Niño region off the west coast of South America (Niño 1+2 SST region) (Lyon and Barnston 2005). The atmosphere failed to couple with SST conditions until late in the austral summer when in February 2005, the SOI reached its lowest level since the 1982–1983 event (Lyon and Barnston 2005). Interestingly, this weak El Niño was detected by the Niño 3.4 SST index for at least six months, while the Niño 3 SST index (commonly used to calibrate ENSO proxy records) only indicated anomalous conditions for 1–2 months (Lyon and Barnston 2005).

The non-stationary nature of ENSO has considerable implications for reconstructing past ENSO events (Gergis et al. 2006). Proxies from a number of ENSO-influenced locations display substantial differences in the seasonality of response signatures. As a result, data from many regions are needed to adequately capture the spatial variability of ENSO through time (Gergis et al. 2006). As such, representation of ENSO signals from a number of widely-spaced regional proxies is more likely to be representative of large-scale ocean-atmosphere processes than is possible from single proxy analysis (Baumgartner et al. 1989; D’Arrigo et al. 1994; Diaz and Pulwarty 1994; Gedalof and Mantua 2002; Gergis et al. 2006; Wilson et al. 2006).

ENSO reconstruction is further complicated by the fact that proxies are not uniformly accurate in recording their local climate or oceanographic environment, and sometimes the narrow seasonal response of climate-sensitive proxies may not coincide with the seasonality of the local ENSO teleconnection (Stahle et al. 1998). For example, a ‘perfect’ proxy would have a constant relationship with local climate that has remained stable through time, allowing each ENSO event to be systematically expressed as a function of tree-ring/coral growth and/or ice accumulation rates. In reality, non-stationarities in ENSO behaviour, proxy-dating issues and inconsistencies in El Niño/ La Niño phase sensitivity. This influences the ratio of accurately detected ENSO events relative to misidentified event years (‘false positive’ cases).

## 2 Rationale for a ‘multi-proxy’ approach to ENSO reconstruction

Each type of proxy represents unique signals from different regions of the globe (tropics versus extra tropics) and environmental contexts (terrestrial versus marine environments), allowing complementary information on the widespread nature of ENSO event signatures to be investigated. The limitations and biases of each proxy are fairly well understood (Jones and Mann 2004). These include differences in temporal resolution (seasonal–annual), and limitations in temporal coverage; a few centuries for corals and historical documentary sources, to thousands of years for tree-ring and ice core sequences (Jones and Mann 2004). Moreover, a proxy climate record is typically only sensitive to a specific seasonal window, rarely captures more than 50% of instrumental variance, and commonly is unable to register variance equally well across a number of frequency domains (Bradley 1996).

The most widely used approach to the reconstruction of ENSO indices involves Principal Component Analysis (PCA), or the equivalent Empirical Orthogonal Function (EOF) techniques (Gergis et al. 2006). To date, reconstructive efforts have tended to focus on only one aspect of the ENSO phenomenon, commonly the Southern Oscillation Index (SOI) (Stahle et al. 1998) or oceanic Niño 3 SST region (Mann et al. 1998, 2000; D’Arrigo et al. 2005). Stahle et al. (1998) were the first to use extensive tree-ring data from south-western USA, Mexico and Indonesia to experimentally reconstruct the Southern Oscillation. Most recently, using an expanded and updated version of the Stahle et al. (1998) data, D’Arrigo et al. (2005) reconstructed December to February Niño 3 SSTs. Using a subset of the Mann et al. (1998) multi-proxy data base, a reconstruction of October to March Niño 3 SSTs for the period A.D. 1650–1980 was developed by Mann et al. (2000). Details of these reconstructions are reviewed by Gergis et al. (2006).

An alternative to the continuous, multivariate regression approaches to ENSO reconstruction are discrete event analyses, typified by the historical chronologies of El Niño events first compiled by Quinn et al. (1987) (Gergis et al. 2006). Following on from this pioneering paper, only a few attempts have been made to expand chronologies of individual ENSO events for the pre-instrumental period (Quinn and Neal 1992; Whetton and Rutherford 1994; Allan and D’Arrigo 1999; Ortlieb 2000). Such records provide a year-by-year chronology of unusual meteorological and hydrological characteristics of discrete ENSO events conditions such as the failure of anchovy fisheries, extreme flooding or drought conditions (Quinn et al. 1987; Whetton and Rutherford 1994).

The ENSO chronology of eastern hemisphere teleconnections compiled by Whetton and Rutherford (1994) and Whetton et al. (1996) attempted to document both phases of ENSO for pre-instrumental times (Allan and D’Arrigo 1999; Ortlieb 2000). To date, no other similar chronology of La Niña events has been compiled. Along with the Quinn and Neal (1992) chronology, Whetton and Rutherford (1994) and Whetton et al. (1996) reconstructed ENSO using four other proxy records from the eastern hemisphere (an Indonesian tree-ring record from Java, the Nile flood record, an Indian drought chronology, and a North Chinese rainfall index). Due to inadequate long-term data coverage, the ENSO chronology and teleconnection stability analysis were restricted to the AD 1701–1979 period (Whetton and Rutherford 1994). Although useful, Whetton and Rutherford (1994) and Whetton et al. (1996) only document extreme (standard deviation defined) ENSO events,

and the La Niña aspect of the chronology is just based on three records (Java, Nile, and China), two of which originate from peripheral teleconnection zones.

The aim of this paper is to use a more comprehensive data set to expand the spatial and temporal replication of the extreme ENSO event chronology assembled by Whetton and Rutherford (1994). Unlike the general overview provided by Gergis and Fowler (2006), this paper introduces an extensive percentile-based methodology for reconstructing (weak, moderate, strong, very strong and extreme) ENSO events back to A.D. 1525. Novel techniques for quantifying reconstruction quality and event magnitudes are also presented for both El Niño and La Niña phase. Finally, changes in the frequency, duration and magnitude of ENSO events are discussed, allowing 20th century ENSO to be evaluated in the context of the past five centuries.

### 3 Data

#### 3.1 Defining ENSO using instrumental indices: the Coupled ENSO Index (CEI)

To calibrate each proxy record, we make use of the Coupled ENSO Index (CEI) of Gergis and Fowler (2005). The CEI is a composite index for the identification of both atmospheric (Southern Oscillation Index) and oceanic (Niño 3.4 region SST) anomalies. Using the indices detailed above, the CEI time series was developed by adding monthly SOI values and monthly Niño 3.4 SST anomalies (multiplied by -1 to allow warm SST values to directionally correspond to low SOI values, indicating El Niño conditions). Anomalies expressed in only one of the two composite indices (indicating decoupled and/or lead/lag ENSO characteristics) are maintained in the CEI, while coupled ocean–atmospheric anomalies result in the amplification of ENSO conditions indicated by the CEI. In addition, monthly classifications of each SOI and SST component are preserved using the classification scheme detailed in Gergis and Fowler (2005).

The CEI is a long time series specifically designed for palaeoclimate applications. The Multivariate ENSO Index (MEI) of Wolter and Timlin (1993), which combines six variables from the ocean–atmosphere domain (1950–present), was considered too short for statistically significant palaeoclimatic calibration (Gergis and Fowler 2005). As some of the records shown in Table 1 terminate in the late 1970s to mid-1980s, the MEI did not provide enough overlap with the instrumental record. Although the CEI does not contain as many variables as the MEI, it is an improvement on the sole atmospheric (SOI) or oceanic (often Niño 3 SST) indices commonly used in ENSO reconstruction (see Gergis and Fowler 2005 for further discussion).

Moreover, since the CEI maintains information about ENSO components, the decoupled (i.e. ocean or atmosphere only) events and lead/lag event signatures from proxy records is possible. Here, we define an ENSO event from the CEI as at least six months of simultaneous oceanic and atmospheric anomalies, with no more than two consecutive neutral months. This is consistent with other definitions found elsewhere in the literature (Trenberth 1997; Allan and D'Arrigo 1999; Hanley et al. 2003).

#### 3.2 Palaeoclimate data

Proxies used in this study (Fig. 1) are predominately published records from core ENSO or key teleconnection areas previously identified as containing an 'ENSO

**Table 1** Proxy records used in this study

<i>Proxy Record</i>	<i>Dates (A.D.)</i>	<i>Data filter</i>	<i>ENSO Zone</i>	<i>CEI-Seasonal sensitivity</i>	<i>Proxy Climate Variable</i>
<b>Tree-rings</b>					
Berlage Indonesian Teak <sup>a</sup>	1525–1929	10-year Gaussian	West Pacific	SON	Total Ring-Widths
D'Arrigo Indonesian Teak <sup>b</sup>	1841–1995	20-year Spline	West Pacific	SON	Total Ring-Widths
New Zealand Kauri <sup>c</sup>	1525–2002	20-year Spline	West Pacific	SON	Total Ring-Widths
New Zealand Pink Pine <sup>d</sup>	1525–1998	20-year Spline	West Pacific	JJA	Total Ring-Widths
Mexican Douglas Fir <sup>e</sup>	1525–1998	20-year Spline	East Pacific	DJF	Total Ring-Widths
SW USA Pinyon Pine <sup>f</sup>	1525–2000	20-year Spline	East Pacific	DJF	Total Ring-Widths
<b>Coral</b>					
Great Barrier Reef <sup>g</sup>	1612–1985	3-year Gaussian	South-west Pacific	DJF	Luminescence SSS
New Caledonia <sup>h</sup>	1658–1992	3-year Gaussian	South-west Pacific	SON	$\delta O^{18}$ SST
Galapagos Islands <sup>i</sup>	1607–1982	3-year Gaussian	East Pacific	DJF	$\delta O^{18}$ SST
Rarotonga <sup>j</sup>	1726–1997	3-year Gaussian	Central Pacific	DJF	Sr/Ca SST
<b>Ice</b>					
Quelccaya Ice Core <sup>k</sup>	1525–1984	3-year Gaussian	East Pacific	DJF	Net annual accumulation

**Table 1** (continued)

<i>Proxy Record</i>	<i>Dates (A.D.)</i>	<i>Data filter</i>	<i>ENSO Zone</i>	<i>CEI-Seasonal sensitivity</i>	<i>Proxy Climate Variable</i>
<b>Documentary Records</b>					
Quinn/Ortlieb <sup>1</sup>	1525–1987	N/A	East Pacific	JJA	Rainfall
Nile <sup>m</sup>	1587–1984	10-year Gaussian	North Africa Teleconnection	MAM	Rainfall
India Drought <sup>n</sup>	1525–1984	N/A	South Asia Teleconnection	SON	Rainfall
China <sup>o</sup>	1525–1979	10-year Gaussian	North Asia Teleconnection	DJF	Rainfall

<sup>a</sup>Berlage (1931), Murphy and Whetton (1989), Whetton and Rutherford (1994), Whetton et al. (1996)

<sup>b</sup>D'Arrigo et al. (1994), IGBP Pages/WDC-A for Paleoclimatology Contribution Series 1999-063

<sup>c</sup>Fowler et al. (2000, 2004, 2008), Fowler (2008), (Gergis et al. 2005a,b)

<sup>d</sup>Fenwick (2003)

<sup>e</sup>Cleaveland et al. (2003)

Stahle and Cleaveland (2002), IGBP Pages/WDC-A for Paleoclimatology Contribution Series 2002-004

Greybill (1994) IGBP Pages/WDC-A for Paleoclimatology Contribution Series 1994-003

Grissino-Mayer and Sweinam (1992) IGBP Pages/WDC-A for Paleoclimatology Contribution Series 1992-012

Dean (1993) IGBP Pages/WDC-A for Paleoclimatology Contribution Series 1993-021

Grow (2000) IGBP Pages/WDC-A for Paleoclimatology Contribution Series 2003-094

<sup>f</sup>Stahle et al. (1998), IGBP Pages/WDC-A for Paleoclimatology Contribution Series 2002-004

<sup>g</sup>Hendy et al. (2003), IGBP Pages/WDC-A for Paleoclimatology Contribution Series 2002-009

<sup>h</sup>Quinn et al. (1998), IGBP Pages/WDC-A for Paleoclimatology Contribution Series 1999-003

<sup>i</sup>Dunbar et al. (1994), IGBP Pages/WDC-A for Paleoclimatology Contribution Series 1994-013

<sup>j</sup>Linsley et al. (2000), IGBP Pages/WDC-A for Paleoclimatology Contribution Series 2000-065

<sup>k</sup>Thompson L (1992) IGBP Pages/WDC-A for Paleoclimatology Contribution Series 1992-008

<sup>l</sup>Quinn and Neal (1992), Ortlieb (2000)

<sup>m</sup>Hassan (1981), Whetton and Rutherford (1994), Whetton et al. (1996)

<sup>n</sup>Whetton and Rutherford (1994), Whetton et al. (1996)

<sup>o</sup>Wang and Zhao (1981), Whetton and Rutherford (1994), Whetton et al. (1996)

\*Berlage Indonesian Teak sequence used from 1525 to 1929, D'Arrigo Teak used from 1930 to 1995. Raw tree-ring widths could not be obtained for the Berlage record, obstructing the development of a single teak chronology for Java. CEI-seasonal sensitivity refers to the period of strongest agreement with the CEI of Gergis and Fowler (2005). Proxy locations are shown in Fig. 1

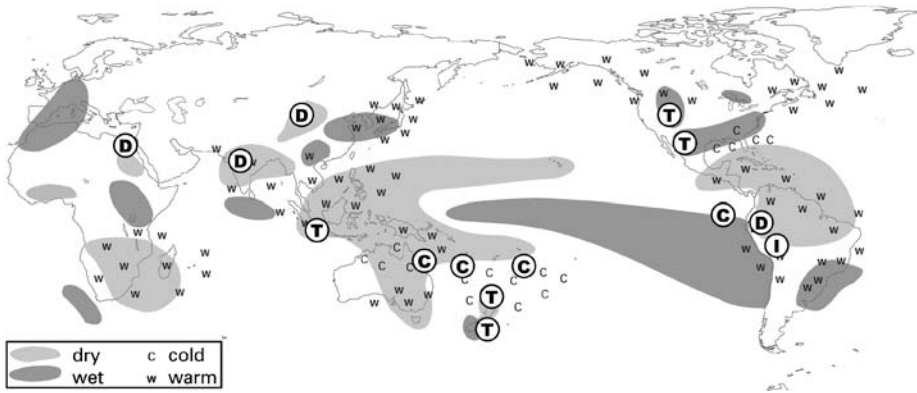


**Fig. 1** Location of proxy records used in this study shown with regard to El Niño teleconnection characteristics. Rainfall anomalies are represented light grey shading (dry) and dark shading (wet). Temperature anomalies indicated by ‘c’ (cool) and ‘w’ (warm) annotation. ‘T’ denotes tree-ring chronologies, ‘C’ coral sequences, ‘D’ documentary record of drought or flood and ‘I’ ice-core data. Details of each record are listed in Table 1. El Niño teleconnection base-map adapted from Allan et al. (1996)

signal’ from both eastern and western Pacific locations back to AD 1525 (Table 1). Coral sequences were limited to those with sufficient, continuous record length and to those given a positive assessment by Lough (2004). This resulted in several shorter and/or discontinuous coral records being excluded from this analysis (Cole et al. 2000; Urban et al. 2000; Cobb et al. 2003).

Although a number of the records listed in Table 1 extend well beyond A.D. 1525 (e.g. the Quelccaya ice core data and all tree-ring records except for the Indonesian Teak) lack of long-term coral data from tropical regions, makes it difficult to establish evidence of global teleconnections associated with ENSO events (Whetton and Rutherford 1994; Grove and Chappell 2000). Accordingly, we limit our analysis to the AD 1525–2002 period.

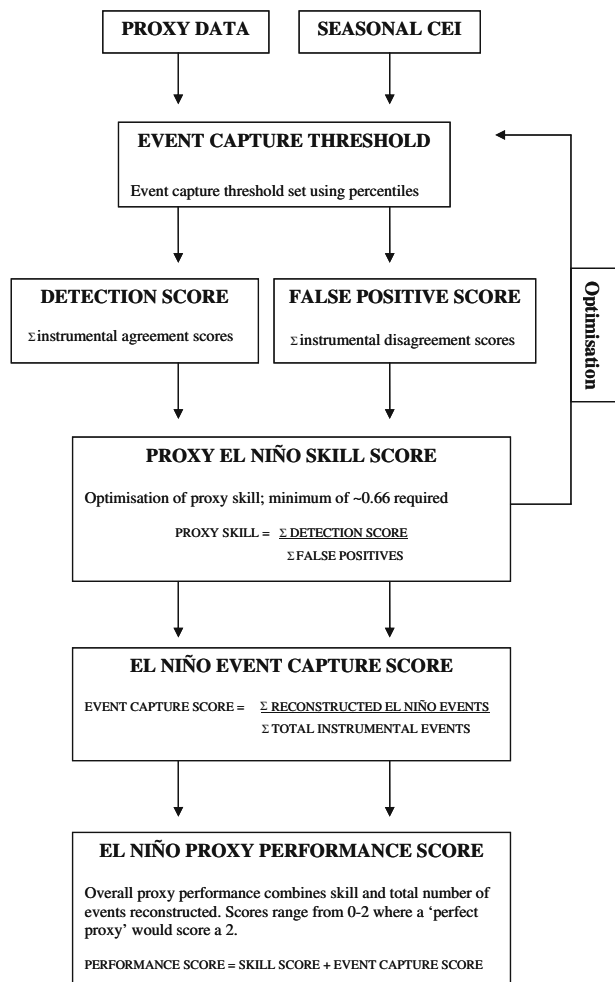
With the exception of the kauri, pink pine and teak, raw tree-ring data was obtained from NOAA’s World Data Center-A for Paleoclimatology. The kauri, pink pine and Berlage teak records were sourced via personal communication (Whetton and Rutherford 1994; Fenwick 2003; Fowler et al. 2004, 2008). All tree-ring sequences (except the Berlage Teak record) were standardised using the program ARSTAN (Holmes et al. 1986) to remove the effects of biological growth for climate analysis. Tree-ring data was filtered using a smoothing spline with 50% variance cut off at 20 years, suitable for high-frequency ENSO analysis, but precluding the analysis of low frequency trends (Fowler and Boswijk 2003). To overcome site-specific biases inherent to individual localities, standardised series for a given species were combined into tree means and then averaged to produce a regional ‘master chronology’ using the tree-ring chronology development software of Fowler and Boswijk (2003).

The Berlage teak record used in this study is a version of the Berlage (1931) chronology modified by Murphy and Whetton (1989). Biological trends in the composite tree-ring series were removed using a linear-logarithmic approximation to produce a tree-ring index series with approximately zero mean (Murphy and

Whetton 1989). The tree-ring index was then filtered to remove long-period fluctuations using a 10-year Gaussian filter, as was done for the Nile and North Chinese Rainfall records (also supplied by Whetton and Rutherford). The historical Indian drought and Quinn chronologies required no further treatment due the event-based nature of the data.

Since ENSO events generally last for one or two years, all coral and ice-core records were smoothed using 3 and 5-year Gaussian filters to attenuate inter-annual noise. Using the process outlined in Fig. 2, a sensitivity analysis was performed to assess the influence of filter window length on instrumental event capture. Results (not shown) indicated that (i) the 3-year filter gave the best match with the ENSO events observed in the instrumental record and (ii) the five-year filter smoothed too much of the inter-annual variability required for high frequency ENSO event analysis. This is consistent with techniques detailed elsewhere in the palaeoclimate literature (Whetton and Rutherford 1994; Diaz and Markgraf 2000; Goodwin

**Fig. 2** Method for calibrating single proxy records to instrumental El Niño events represented by seasonal Coupled ENSO Index (CEI) event classification (Gergis and Fowler 2005). The same procedure was followed for La Niña calibration



et al. 2004; Linsley et al. 2004; Lough 2004; D'Arrigo et al. 2005). Note that this results in the loss of mean decadal-centennial trends, preventing the analysis of low frequency changes in ENSO phase. The primary intention of this paper is, however, to document changes in the frequency and magnitude of inter-annual ENSO events.

## 4 Methods

### 4.1 Single proxy calibration

Figure 2 outlines the methodology involved in calibrating single proxy records to observed ENSO events. Similar to the approach of Mann et al. (2000), we do not make use of any *a priori* seasonal window for calibration purposes, in recognition that proxy indicators vary considerably in the timing of climate-related anomalies. The seasonal ENSO classifications of Gergis and Fowler (2005), which maintain information about separate SST and SOI conditions, are used to identify the season which expressed the strongest ENSO signal within a given proxy record (shown in Table 1). This allowed decoupled events (i.e. events only registered by the atmosphere or ocean but not experienced simultaneously by both) to be analysed (Gergis and Fowler 2005).

Event capture thresholds were iteratively adjusted to achieve the highest skill score for each CEI season (Fig. 2). A 'detection score' of 1 was assigned each time a proxy response accurately corresponded to instrumental ENSO conditions (detection score). Since ENSO exhibits periodic decoupling of SOI and SST anomalies (Deser and Wallace 1987; Gergis and Fowler 2005), half weight scores were applied when the proxy agreed with only one ENSO component (atmospheric or SST conditions). Note that the skill score was optimised separately for each ENSO phase.

To quantify the uncertainty associated with event detection, misidentified cases, or false positives, were also quantified to further assess proxy skill (Fig. 2). False positives are defined here as a proxy exhibiting a response conflicting with instrumental conditions, for example, a CEI El Niño corresponding to an apparent La Niña proxy response, or vice versa. In this case, a score of  $-1$  was assigned.

Finally, the detection score and false positive score were divided to provide a simple measure of 'proxy skill'. The calibration process was designed to achieve a high signal (detection score) to noise (false positive score) ratio by not allowing the proportion of false positive cases to exceed  $\sim 33\%$ . This corresponds to a skill score of approximately 0.66, indicating a 2/3 chance of accurate event detection by a proxy. Although this is somewhat arbitrary, it was considered to be a more conservative target than a 50/50 split of event 'hits and misses'.

To provide a complete assessment of each proxy's reconstruction potential, the proportion of instrumental CEI events captured by a given proxy ('event capture score') was added to the proxy skill score to produce an overall 'proxy performance score' (Fig. 2). This accounts for the fact that some proxies may, for example, be excellent at only picking up extreme events. But how useful is a proxy that only captures a low percentage of the total events in the observational record? Ideally a proxy should pick up as many events as accurately as possible (i.e. high 'proxy skill' and a high 'event capture score').

Hypothetically, a ‘perfect proxy’ would have a proxy performance score of two (all events captured accurately), while a proxy with no ENSO skill would score a zero. After selecting the optimal percentile thresholds for each proxy (for each ENSO phase), records were ranked by their overall proxy performance score to indicate their usefulness for El Niño, La Niña or both phases of the reconstruction. The percentile thresholds identified as producing the best skill score in the instrumental period were then applied to the remainder of the proxy data to identify pre-instrumental ENSO signatures.

Table 2 provides an example of the calibration process for the Great Barrier Reef coral record. Following the methodology of Fig. 2, a variety of percentile threshold values are set until for each phase. From Table 2 it can be seen that a threshold is reached beyond which no improvement in the instrumental event capture score is achieved for each phase. Indeed, there is a decline in the overall proxy skill as the proportion of false positives increases suggesting a compromise between the number of events captured and the accuracy (or ‘skill’ with which they are detected) is required. A very high proxy skill score of 0.81 is possible using the 10th percentile threshold for the El Niño calibration; however, relatively few observed events (19%) are registered.

From Table 2, it is apparent that aiming for a proxy skill score of least  $\sim 0.66$  appears to be a reasonable target that allows sufficient sensitivity to event capture, reflected in the proxy performance score. In this hypothetical example, an overall proxy performance score of 1.07 for the El Niño and 1.27 for La Niña phase would be selected to calibrate the Great Barrier Reef coral record for past ENSO reconstruction. Due to the inherent replication implicated by multi-proxy analysis, maximising the event capture at the single proxy level was desired, as false positives are likely to be ‘lost’ from the larger, multi-proxy environment as the likelihood of false positives occurring simultaneously in many locations is likely to be low.

**Table 2** Impact of skill score optimisation process on the Great Barrier Reef coral record

Percentile Threshold	Detection Score	False positives Score	Proxy Skill Score	Instrumental Event Capture Score	Proxy Performance Score
<i>El Niño</i>					
10th	5.5	1.0	0.81	0.19	1.00
15th	9.0	2.0	0.77	0.30	1.07
20th	10.5	3.5	0.67	0.33	1.00
25th	12.0	6.0	0.50	0.37	0.87
30th	14.0	8.5	0.39	0.44	0.83
35th	16.5	9.0	0.45	0.48	0.93
<i>La Niña</i>					
65th	23.0	8.0	0.65	0.62	1.27
70th	20.0	7.0	0.65	0.53	1.18
75th	15.5	6.5	0.58	0.41	0.99
80th	13.0	6.0	0.53	0.35	0.88
85th	11.5	4.0	0.65	0.32	0.97
90th	7.5	3.0	0.60	0.21	0.81

The process is aimed at maximising instrumental event capture (expressed as a decimal) while maintaining a high degree of skill, determined from the period of instrumental overlap, 1871–1985. Note the greater La Niña phase sensitivity in this example. An overall proxy performance score of 1.07 for the El Niño and 1.27 for La Niña phase were selected

## 4.2 Identifying ENSO events using multiple proxy records

After assessing single proxy records it was apparent that each proxy displayed considerable differences in ENSO phase sensitivity, demonstrated in Table 2. This highlighted the need to verify the occurrence of an ENSO episode using a number of palaeo-environmental sources. Attempting to identify ENSO events using multiple proxy records immediately raises a number of key questions including:

1. How does the loss of records (replication) through time impact the overall reconstruction?
2. Should ENSO reconstruction be separated based on phase sensitivity?
3. How does proxy skill influence the reliability of any reconstruction?
4. How many records are needed to accurately reproduce observed ENSO events?
5. Can proxy skill adequately compensate for the loss of records back in time?
6. Is a reconstruction based on fewer records with higher proxy skill more useful than a reconstruction based on a better-replicated network of records with lower proxy skill?

These issues can be summarised as the two fundamental issues of (i) replication and (ii) proxy skill, and are further detailed below.

### 4.2.1 Replication

Few proxy records extend back more than a few centuries resulting in an inevitable degradation of the quality of any reconstruction back through time as replication diminishes. This is especially the case in the context of the wider multi-proxy network, as the representation of long records decreases back in time (Fig. 3). Thus, most confidence can be placed on the period containing the most records. Nevertheless, in this study eight (six) El Niño (La Niña) proxies are present in the reconstruction back to A.D. 1525. As the number of proxies analysed through time fluctuates there may be inflation (under-estimation) in the occurrence of an event due to higher (lower) relative numbers of available proxy records. Reconstruction quality, however, is likely to reflect the overall skill of the subset of proxies contributing to the reconstruction for each year.

Following the calibration of single proxy records, a sensitivity analysis was undertaken to explore the number of proxies (replication) needed to maximise ENSO event capture (while minimising false positive cases) in a multi-proxy context during the instrumental period (1871–2002). This was carried out on subsets of El Niño and La Niña sensitive proxies with skill scores exceeding 0.66. This allowed the degree of uncertainty associated with defining an ENSO event based on a minimum requirement of three proxies to over seven proxies in terms of correct event capture, false positive cases, decoupled and missed events to be quantified. This provided a basis for assessing the potential of over/under reconstruction of ENSO events in the pre-instrumental period. Unlike Whetton and Rutherford (1994), any combinations of proxies were used for ENSO event definition since teleconnection non-stationarities are known to exist (Stahle et al. 1998; Mann et al. 2000; Hendy et al. 2003; Power et al. 2006).

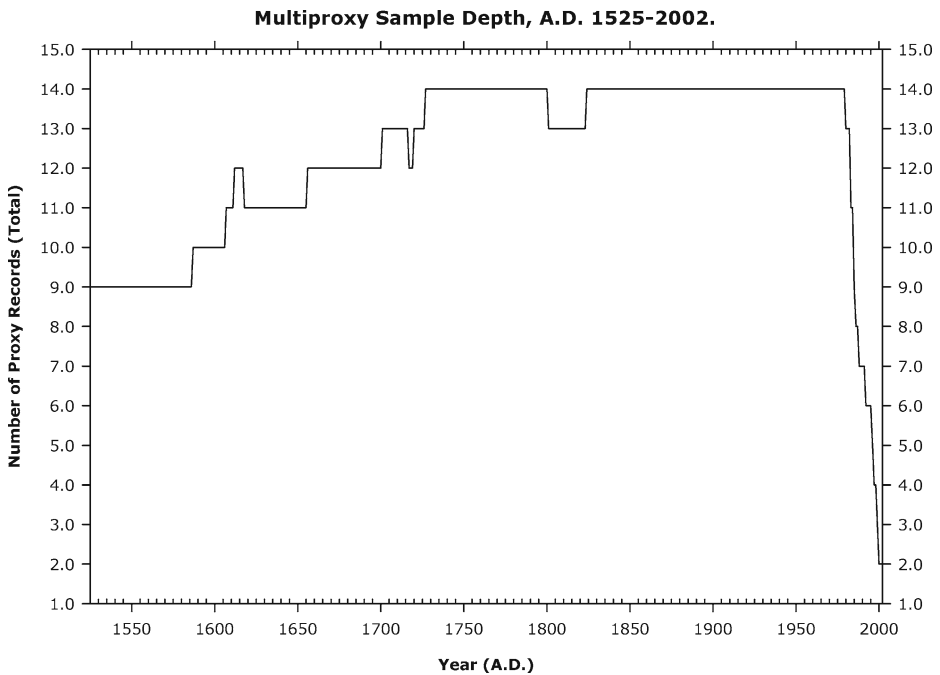


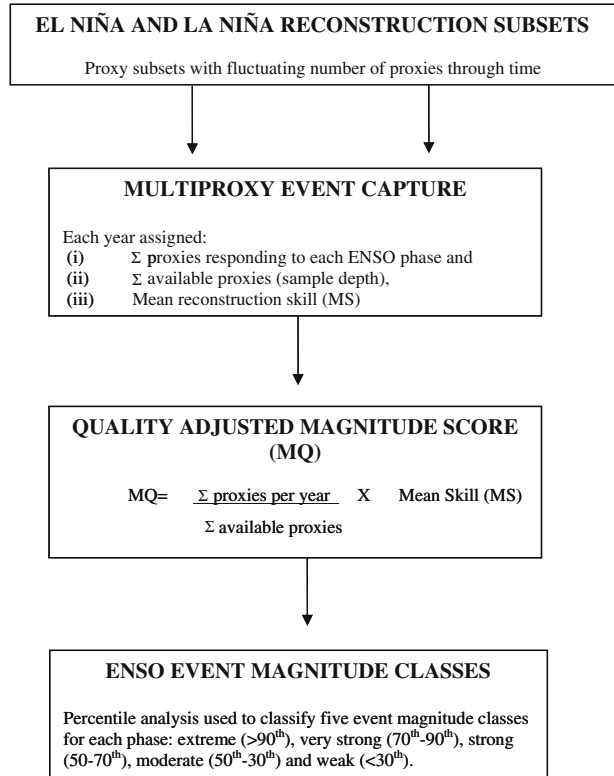
**Fig. 3** Multi-proxy sample depth, A.D. 1525–2002. Prominent sample depth (number of available proxies) fluctuations are due to a) various gaps in the Nile flood data, b) loss of temporal coverage of coral sequences, c) post-1900 gaps in the Galapagos coral record and d) only seven records covering the 1990s

#### 4.2.2 Proxy skill

To allow the skill of the proxy to be incorporated into the quantification of event magnitude, a quality adjusted magnitude (MQ) time series was devised (Fig. 4). Firstly, the mean reconstruction skill score (MS) was developed to indicate the general quality of the subset of proxies contributing to the reconstruction at a given point in time. The relative proportion (rather than total number) of ENSO responsive records was then multiplied by the MS score for each year to allow the weight of the best proxies to be inherently recognised in the MQ score. This addresses the issue of a loss of records through time.

To define the intensity and quality of reconstructed events, a percentile analysis on the MQ time series was then performed to isolate extreme, very strong, strong, moderate and weak El Niño (La Niña) conditions. This was achieved by selecting five percentile classes based on calibrating the multi-proxy network response to match historical strong-extreme events identified by Trenberth (1997) and Gergis and Fowler (2005) during the instrumental (1871–2002) period. Five event classes ranging from extreme (>90th percentile) very strong (70th–90th percentile), strong (50th–70th), moderate (50th–30th) and weak events (<30th) identified from the instrumental period were then applied to the quality adjusted magnitude time series back to A.D. 1525. Our definition of an extreme event is consistent with that used by Working Group 1 of the Intergovernmental Panel on Climate Change (IPCC) (Trenberth et al. 2007).

**Fig. 4** Outline of ENSO event quality-adjusted magnitude (MQ) index. Amplitude of ENSO events are relative to the corresponding number of proxy records available for each phase. The same process was repeated for the A.D. 1525 sub-sample analysis described in Section 4.2.3



#### 4.2.3 A.D. 1525 sub-sample analysis

A subset analysis was done to assess if a loss of records (proxy replication) reduces the reliability of our ENSO reconstructions back in time. To do this, the methodology outlined in Fig. 4 was applied to the subset of El Niño and La Niña proxies available continuously back to A.D. 1525. Comparisons of the event capture, magnitude and reconstruction quality characteristics of the A.D 1525 subset reconstructions were made against the reconstructions based on the *complete* proxy network. To further assess whether the overall skill of a proxy subset is sufficient to compensate for the loss of records back in time, correlations between the mean reconstruction skill (MS) and quality-adjusted magnitude (MQ) time-series (Fig. 4) were calculated in 50-year intervals.

## 5 Results

### 5.1 Single proxy calibration

Results of the proxy calibration analysis are shown in Table 3. Of the 15 records analysed, 12 (9) records achieved an El Niño (La Niña) skill score of  $\geq 0.66$ . However for La Niña this rose to twelve if the skill score criterion was relaxed to a minimum

**Table 3** Proxy calibration results for El Niño (top) and La Niña (below) phase reconstruction ranked in relation to overall proxy performance score (last column)

	<b>Record Type</b>	<b>Percentile Threshold</b>	<b>Detection Score</b>	<b>False Positive Score</b>	<b>Proxy Skill Score</b>	<b>CEI Event Capture (%)</b>	<b>Proxy Performance Score (Skill &amp; Event Capture)</b>
<b><i>El Niño</i></b>							
Mexico	Tree-ring	59th	31.0	-7.5	0.76	81.25	1.57
Quinn	Documentary	65th	24.5	-6.0	0.76	74.07	1.50
India	Documentary	65th	14.0	-0.5	0.96	48.15	1.45
Berlage Teak	Tree-ring	30th	8.0	-1.5	0.81	60.00	1.41
Kauri	Tree-ring	74th	23.0	-6.0	0.74	60.61	1.36
Quelccaya	Ice Core	70th	19.5	-6.0	0.69	62.96	1.32
SW USA	Tree-ring	63rd	24.5	-9.5	0.61	59.38	1.21
Rarotonga	Coral	74th	16.5	-4.5	0.73	45.16	1.18
D'Arrigo Teak	Tree-ring	29th	15.0	-5.0	0.67	48.39	1.15
Pink Pine	Tree-ring	27th	18.5	-6.0	0.68	44.12	1.12
Galapagos	Coral	25th	12.5	-5.0	0.60	50.00	1.10
Nile	Rainfall	20th	11.5	-3.5	0.70	32.14	1.02
Great Barrier Reef	Coral	16th	10.0	-2.0	0.80	33.33	1.13
China	Rainfall	90th	5.5	-1.5	0.73	19.23	0.92
New Caledonia	Coral	93rd	4.5	-2.0	0.56	10.34	0.66

**Table 3** (continued)

		<b>Record Type</b>	<b>Percentile Threshold</b>	<b>Detection Score</b>	<b>False Positive Score</b>	<b>Proxy Skill Score</b>	<b>CEI Event Capture (%)</b>	<b>Proxy Performance Score (Skill &amp; Event Capture)</b>
<b><i>La Niña</i></b>								
Berlage Teak		Tree-ring	59th	12.5	-3.5	0.72	69.23	1.41
SW USA		Tree-ring	38th	27.5	-7.5	0.73	63.16	1.36
Mexico		Tree-ring	42nd	28.0	-8.0	0.71	63.89	1.35
Great Barrier Reef		Coral	65th	23.0	-8.0	0.65	61.76	1.27
Nile		Rainfall	86th	9.5	-2.5	0.74	50.00	1.24
Pink Pine		Tree-ring	27th	20.5	-7.0	0.66	54.17	1.20
Kauri		Tree-ring	37th	23.5	-7.5	0.68	52.50	1.20
D'Arrigo Teak		Tree-ring	29th	22.5	-9.0	0.60	58.33	1.18
New Caledonia		Coral	93rd	22.5	-8.0	0.64	51.43	1.16
Galapagos		Coral	25th	5.5	-1.0	0.82	31.82	1.14
Rarotonga		Coral	74th	15.5	-4.5	0.71	38.89	1.10
Quelccaya		Ice Core	70th	15.0	-4.5	0.70	38.24	1.08
China		Rainfall	26th	14.0	-7.5	0.46	34.29	0.81

Note that a lower skill score of  $\sim 0.6$  was needed for three La Niña proxies; D'Arrigo Teak (0.6), Great Barrier Reef (0.65) and New Caledonia (0.64), to allow a similar number of records to be included in each ENSO phase reconstruction

skill of 0.6. In an attempt to address this bias, this slightly lower threshold was adopted for three La Niña proxies (D'Arrigo Teak (0.6), Great Barrier Reef (0.65) and New Caledonia (0.64)) to allow a similar number of records into each ENSO phase reconstruction. The slight bias towards El Niño sensitivity of proxy records is reflected in the overall skill and proxy performance scores shown in Table 3.

El Niño skill scores ranged from 0.56 for New Caledonia coral to a high 0.96 for the Indian drought chronology. When considering overall proxy performance, Mexico, Berlage Teak and Kauri are the most useful tree-ring records, while the Quinn record and Indian drought chronology also rank second and third in terms of reconstruction importance. Rarotonga coral record appears in the top ten El Niño proxies, with the Quelccaya ice-core performing better than any of the coral records. Clearly, the Nile, China and New Caledonian coral are not strong overall performers for El Niño reconstruction.

The Chinese record had the lowest La Niña skill score (0.46) and the Galapagos coral sequence the highest (0.82). The Berlage Teak sequence from Indonesia is the overall best performing tree-ring record, followed by the southwest USA, and Mexican tree-ring chronologies. The Great Barrier Reef record was the best performer of the coral sequences. With the exception of the Great Barrier Reef record, the other coral sequences do not rank highly in terms of their La Niña event sensitivity. Low La Niña sensitivity was also observed from the Quelccaya ice-core record from Peru.

Single-phase sensitivity was noted for a number of proxies. La Niña sensitivity was observed for proxies from New Caledonia, southwest USA and the Galapagos, while single El Niño-phase sensitivity was noted in the Chinese rainfall, Quinn record, and Indian drought records. Dual-phase sensitivity was noted for all the tree-ring records (with the lesser La Niña sensitivity of D'Arrigo Teak record noted above), the two coral records from Rarotonga and Great Barrier Reef and the Quelccaya ice-core. It is worth recognising, however, that it is possible that phase-sensitivity results reported here reflect the essentially arbitrary threshold selection of the methodology employed here. This is an inherent bias common to all proxy reconstructions.

## 5.2 Multi-proxy calibration

### 5.2.1 Proxy replication sensitivity analysis

To investigate the impact of proxy replication on ENSO event reconstruction, an analysis of the frequency and duration characteristics is presented in Table 4. Raising the proxy-replication threshold from three to seven records reduced both the overall event capture and false positive 'misfires' (detailed further in Table 5). Generally, as more stringent proxy replication thresholds are imposed, event capture decreases discernibly as does mean event duration. Furthermore, it was clear that increasing the number of proxies used to replicate an ENSO event signature was indicative of the magnitude of an event. Logically, highest confidence in the reconstruction was found to be associated with events of a stronger magnitude when there is a high degree of replication of the climate signal in various proxies (see Table 5).

For the El Niño reconstruction, there are minor differences in the frequency of events using a three or four proxy replication threshold for the instrumental period, ranging from 22 to 27 reconstructed events (Table 4). However, in the

**Table 4** Event frequency and duration characteristics for reconstructed instrumental and pre-instrumental periods

Number of Proxy Records	Instrumental Frequency (1871–2002)	Mean/Maximum Duration (Years)	Pre-Instrumental Frequency (1525–1870)	Mean/Maximum Duration (Years)	Total Events (1525–2002)
<b><i>El Niño</i></b>					
≥ 3	27	2.4/8.0	65	1.9/7.0	92
≥ 4	22	2.0/5.0	40	1.3/3.0	62
≥ 5	20	1.5/4.0	18	1.1/2.0	38
≥ 6	8	1.7/4	5	1.0/1.0	13
≥ 7	3	1.3/2	1	1.0/1.0	4
<b><i>La Niña</i></b>					
≥ 3	26	3.1/10.0	56	3.3/36.0 (2.8/11.0)	82
≥ 4	21	2.4/6.0	60	2.0/9.0	81
≥ 5	16	2.3/5.0	36	1.8/8.0	52
≥ 6	15	1.5/3.0	18	1.3/2.0	33
≥ 7	8	1.0/1.0	10	1.0/1.0	18

Note that consecutive event years are classified as a single ENSO event only

pre-instrumental period, where the number of records decreases (see Fig. 3), the implications of using higher thresholds for event definition become apparent. For example, there is a difference of 47 events between using three and five proxy records in the pre-instrumental period.

During the instrumental period, mean El Niño event duration declines from 2.4 years using the three-proxy threshold to 1.3 years using seven-proxy threshold.

**Table 5** Reconstruction quality characteristics associated with each multi-proxy threshold

Number of Proxy Records	Instrumental Event Capture (1871–2002)	Total False Positives (Events)	Decoupled Events (Total)	Missed Events (Total)	Reconstruction Confidence Level (%)
<b><i>El Niño proxies</i></b>					
≥ 3	27	5	4	4	81.5
≥ 4	22	1	3	6	95.5
≥ 5	20	1	2	6	95.0
≥ 6	8	0	1	15	100.0
≥ 7	3	0	0	21	100.0
<b><i>La Niña proxies</i></b>					
≥ 3	26	7	8	1	73.1
≥ 4	21	5	4	4	76.2
≥ 5	16	3	0	7	81.3
≥ 6	15	2	0	8	86.7
≥ 7	9	1	0	14	87.5

False positives are defined here as a proxy exhibiting a response conflicting with instrumental conditions, decoupled events refer to events only registered by the atmosphere or ocean but not experienced simultaneously by both or an event unresolved by a reconstruction subset. Reconstruction confidence level refers to the proportion of false positives relative to accurate instrumental event capture (%) as represented by the CEI of Gergis and Fowler (2005)

Notably, the three-proxy replication threshold maintains the most consistency in mean and maximum event characteristics in both the observed and pre-instrumental period, in addition to a high event capture. Since all replication thresholds give an event count less than the 28 El Niño events noted by Gergis and Fowler (2005) from the instrumental CEI record, the three-proxy replication threshold was considered to have closest agreement with instrumentally observed frequency of events.

For the La Niña reconstruction, three and four-proxy replication thresholds for event definition yield comparable frequency results for the instrumental and pre-instrumental periods. Raising the replication threshold to five proxies reduces instrumental event capture by up to 10 (30) events compared to the three-proxy threshold for the calibration (pre-instrumental) period. Event duration appears over-sensitive for the lowest three-proxy replication threshold, resulting in a maximum duration of 36 consecutive years between A.D. 1738–1773, which may be unlikely. Excluding this protracted event results in a mean (maximum) duration of 2.8 (11) years, which is similar to the three proxy replication threshold duration characteristics noted for the observational period (Table 4).

The four-proxy La Niña threshold appears to maintain fairly consistent mean duration characteristics in both the post-1870 (2.4 years) and pre-instrumental (2.0 years) periods, while maintaining a reasonable overall event capture. The 21 events captured in the observational period compares well to the 26 La Niña episodes identified in the instrumental CEI record (Gergis and Fowler 2005). The similarities of the La Niña event capture noted in the pre-instrumental period for the three and four proxy replication thresholds is a result of the prolonged cool event from A.D. 1863–1875 being split into three separate events (A.D. 1863–1864, 1866–1868, 1870–1875) using the four proxy threshold.

The impact of adjusting the proxy replication threshold is further examined in Table 5. Clearly lowering the minimum proxy threshold for ENSO event definition increases the probability of including false positives in the reconstruction, reflected in lower confidence scores listed in Table 5. For example, there is a notable increase in the number of missed events from a minimum of four to a maximum of 21 events using the three and seven proxy minimum for the El Niño reconstruction. This implies that adopting a lower proxy replication threshold may be more appropriate in the interest of maintaining reconstruction potential from the multi-proxy assemblage.

There is an increase in the capture of decoupled events as a lower threshold is adopted. This increase is more pronounced for the La Niña analysis where lower proxy thresholds result in the reconstruction of a maximum of eight decoupled SOI events (e.g. 1929, 1960, 1981). Importantly, none of the reconstructions for either phase are able to entirely reproduce the instrumentally observed CEI, although considerable skill is still achieved, as seen in Table 5.

The maximum confidence level for the La Niña reconstruction is 87.5% for the seven-proxy replication threshold. The sole false positive case relates to 1953 where an exceptional nine proxies indicate La Niña conditions. That year does not correspond to the 6-month instrumentally observed El Niño that achieved a maximum SST anomaly of 1.13°C. However, La Niña conditions began developing in the SOI by June 1954, culminating in a coupled event spanning August 1954 to March 1955 (not shown). This highlights the potential weaknesses inherent in palaeoclimate reconstruction, and may suggest that proxies were responding to factors other than ENSO at this time.

Since there were minor differences in the event capture characteristics of the three and four-proxy event lists (see Tables 4 and 5), using four proxies for La Niña event definition was considered to be slightly more conservative than a criteria based on a three-proxy replication threshold. Thus, a three (four) proxy replication threshold was adapted for El Niño (La Niña) event definition using our multi-proxy assemblage to resolve the highest degree of events possible from the reconstruction.

### 5.2.2 Reconstruction quality assessment

As noted in Section 4.2.1, the number of proxy records available for ENSO reconstruction fluctuates through time, which may bias the apparent trends seen in the occurrence and magnitude of reconstructed ENSO events. Thus, to investigate the implications of the inevitable loss of records, event capture statistics for the full data set (Table 5) were compared with those for a smaller data set of the proxy subsets available back to A.D. 1525 (Table 6). The 1871–2002 period was used as it is the only interval that can be cross verified with observational ENSO data, represented in this study by the CEI of Gergis and Fowler (2005). Due to growth limitations of coral records, only tree-ring, ice-core and documentary records are available back to A.D. 1525. A good representation of eastern and western Pacific proxies is, however, still maintained (see Table 1).

Table 6 indicates the event capture obtained using the three-proxy replication thresholds between the full and 1525 proxy subsets of the reconstruction for each phase. For both the El Niño and La Niña phase, 96% of events noted in the full reconstruction are present in the subset back to A.D. 1525. This suggests loss of sample depth is not detrimental in event capture using a three-proxy threshold for event definition in the multi-proxy environment.

Raising the replication threshold to four proxies, there is still good agreement for the El Niño phase (90%), however, the La Niña reconstruction suffers from a loss of replication, falling to 81% agreement. Above a four-proxy replication threshold, there is substantial loss in reconstruction potential which is most marked for La Niña phase reconstruction, reflecting the lower overall proxy sensitivity noted in Table 6.

To further assess if the overall skill of a proxy subset is sufficient to compensate for the loss of records back through time, correlations between the mean reconstruction skill (MS) and quality-adjusted magnitude (MQ) (see Fig. 4) were calculated over 50-year intervals. The exception was the A.D. 1525–1550 period where a 25-year interval was used. Table 7 indicates the very high similarity between the complete and 1525 subsets, suggesting sufficient high quality proxies exist at the early end of the reconstruction to overcome quality issues associated with loss of sample depth. MS was found to fluctuate more than MQ for both phases of the reconstruction. The most notable discrepancy was noted for La Niña phase for the A.D. 1701–1750 period when a low correlation of 0.47 was observed. This corresponds to a loss of records noted in Fig. 3, most notably the gaps in the Nile flood record (a key La Niña proxy listed in Table 3), and a loss of coral records at this time.

MQ correlations between the complete and 1525 subsets remain very high for both phases of the reconstruction, however, the relatively lower sensitivity of proxies to La Niña conditions noted in Section 5.1 is again seen in Table 7. The lowest MQ correlation for El Niño (La Niña) phase is noted during A.D.1751–1800 (A.D. 1951–2002) when a correlation of 0.87 (0.81) is noted, most likely reflecting changes in proxy replication. Aside from A.D.1751–1800, differences in the degraded El Niño

**Table 6** Comparison of the A.D. 1525 (degraded) subset and the full reconstruction event capture characteristics as per Table 5 for the instrumental (A.D. 1871–2002) and pre-instrumental (A.D. 1525–1870) periods

Proxy Record Subsets Present at A.D. 1525	Instrumental Event Capture (1871–2002)	Total False Positives (Events)	Decoupled Events (Total)	Missed Events (Total)	Agreement with Total Proxy Subset Event Capture (1871–2002) (%)	Pre-instrumental Event Capture (1525–1870)	Total Event Capture (1525–2002)
<i>El Niño proxies</i>							
≥ 3	26	4	4	4	96.3	66	92
≥ 4	20	1	1	6	90.1	33	53
≥ 5	11	0	1	13	55.0	12	23
≥ 6	1	0	0	22	12.5	2	3
<i>La Niña proxies</i>							
≥ 3	25	3	4	3	96.2	74	99
≥ 4	17	2	1	7	81.0	47	64
≥ 5	6	1	0	16	37.5	13	19
≥ 6	1	0	0	19	6.7	1	2

False positives are defined here as a proxy exhibiting a response conflicting with instrumental conditions, decoupled events refer to events only registered by the atmosphere or ocean but not experienced simultaneously by both and an event unresolved by a reconstruction subset. ‘Agreement with total proxy subset event capture’ refers to the percentage of reconstructed events common between the full and limited A.D. 1525 proxy subsets. Note that the seven proxy replication threshold values are omitted due to low reconstruction potential seen from the six proxy threshold

**Table 7** A comparison of the Mean Skill (MS) and Quality Adjusted Magnitude (MQ) time series (see Fig. 4 for explanation) calculated between the AD

Sub-period	Mean Skill (MS) correlation (r)	Quality Adjusted Magnitude (MQ) correlation (r)
<b><i>El Niño</i></b>		
Full period (1525–2002)	0.97	0.96
1951–2002	0.90	0.97
1901–1950	0.97	0.95
1851–1900	0.98	0.92
1801–1850	0.97	0.95
1751–1800	0.96	0.87
1701–1750	0.95	0.95
1651–1700	0.99	0.99
1601–1650	1.00	1.00
1551–1600	0.99	1.00
1525–1550	0.96	1.00
<b><i>La Niña</i></b>		
Full period (1525–2002)	0.83	0.87
1951–2002	0.86	0.81
1901–1950	0.87	0.87
1851–1900	0.73	0.91
1801–1850	0.73	0.88
1751–1800	0.70	0.84
1701–1750	0.47	0.89
1651–1700	0.88	0.92
1601–1650	0.83	0.92
1551–1600	0.93	1.00
1525–1550	0.96	1.00

1525 subset and full reconstructions in 50-year intervals. Note the exception of the 25-year A.D. 1525–1550 interval

reconstruction appear negligible, remaining above a correlation of at least 0.92. This implies that a loss of replication back in time is not overly detrimental to the reliability of the El Niño reconstruction. Relatively less confidence can be placed on the La Niña phase reconstruction, however, considerable skill is still achieved. It is clear that adjusting for both replication and proxy skill in the MQ time series is more robust measure for assessing reconstruction reliability rather than assessment based on the mean skill (MS) of a proxy subset alone. This suggests that proxy skill may be more important than the overall quantity (replication) of records used for ENSO reconstruction.

### 5.2.3 ENSO event verification results

To further assist the selection of a minimum replication threshold needed for multi-proxy ENSO event definition, the three and four proxy-threshold events were compared to past ENSO event lists published for the instrumental period (Rasmusson and Carpenter 1983; Kiladis and Diaz 1989; Quinn and Neal 1992; Whetton and Rutherford 1994; Mullan 1995; Trenberth 1997; Ortlieb 2000; Allan et al. 1996).

**Table 8** Comparison of multi-proxy event lists based on three and four proxy replication thresholds with published events for verification

ENSO Event Lists	Instrumental Event Capture (1871–2002)	Pre-Instrumental Event Capture (1525–1870)	Total Event Capture (1525–2002)
<b><i>El Niño</i></b>			
≥ 3 Multiproxy events	27	65	92
≥ 4 Multiproxy events	22	40	62
Quinn & Ortlieb (QO00)	29	80	109
Whetton and Rutherford (WR94)	16	23	39
<b><i>La Niña</i></b>			
≥ 3 Multiproxy events	26	59	85
≥ 4 Multiproxy events	21	61	82
Quinn and Ortlieb (QO 00)	–	–	–
Whetton and Rutherford (WR94)	4	6	10

The ‘QO00’ reconstruction (Ortlieb (2000) pre-1901 and Quinn and Neal (1992) for the post-1900 period) and ‘WR94’ (Whetton and Rutherford 1994) ENSO chronologies were used for comparison as they represent the most comprehensive compilations of ENSO events to date. Note that the QO00 chronology does not contain a history of La Niña events

For the pre-instrumental period, two lists provided by the ‘Quinn record’ (Ortlieb 2000 pre-1901 and Quinn and Neal 1992 for the post-1900 period) and Whetton and Rutherford (1994) were used. These chronologies are hereafter referred to as ‘QO00’ and ‘WR94’, respectively. Table 8 shows the event capture characteristics of the two primary long-term ENSO event lists of QO00 and WR94 and the multi-proxy event lists from the analysis presented here. Note that although these records are not independent of the data set analysed here, a general comparison provides a basic indication of the relative improvements in overall event reconstruction.

There is similarity between the El Niño events identified by the QO00 record and the use of three proxies for event definition. The additional 16 events not included in the multi-proxy event lists reported here may indicate El Niño conditions that may have only been regional in nature (e.g. A.D. 1531–1532, 1604, 1624, 1761, 1819). Events from the multi-proxy reconstructions have a longer duration than a number of the events indicated in QO00 (not shown), which may reflect the impact of calibrating proxies using the CEI which allowed lead/lag signatures associated with decoupled events to be resolved. Consequently, the results may be a sign of larger-scale patterns of ENSO events, rather than the response of one (East Pacific) teleconnection region.

Verification of La Niña events was substantially more difficult due to the lack of coverage in the QO00 and a total of ten events noted by WR94. The year A.D. 1906 is the only La Niña event not present in the three or four proxy La Niña chronologies; however, the 1826 La Niña noted by WR94 is only detected using the three-proxy threshold. Since there were minor differences in the event capture characteristics of the three and four-proxy event lists, using four proxies for La Niña event definition was considered to be a slightly more conservative than a criteria based on a three-proxy threshold. Thus, a three (four) proxy replication threshold was adapted for El Niño (La Niña) event definition using our multi-proxy assemblage to resolve the highest degree of events possible from the reconstruction.

### 5.3 Multi-proxy ENSO event definition

#### 5.3.1 Using *MQ* to classify pre-instrumental ENSO

Having ‘tuned’ the reconstructions to reproduce the main features of the observational ENSO record, next the minimum quality adjusted magnitude score (*MQ*) associated with the three (four) proxy replication threshold was used to classify an El Niño (La Niña) event. This provided a minimum quality threshold, allowing events based on fewer, but higher quality proxy records, to be included in the analysis. This was most crucial for the beginning and end of the reconstruction when fewer proxies were available. The appropriate *MQ* minimum thresholds were then applied to the remainder of the time series to identify years where reconstruction quality standards were met, regardless of the total number of proxies replicating an ENSO signal. This allowed the quality *and* level of replication to be used as a basis for event identification (ranging from weak to extreme events), to compensate for lower magnitude decoupled, lead or lag event characteristics (Table 9).

From Table 9, a total of 92 (82) El Niño (La Niña) events were reconstructed since A.D. 1525. Of these, 37 very-strong to extreme El Niño were observed. Nine El Niño events were classified as extreme, including five well-known events of the 20th century (2002, 1982–1983, 1941–1942, 1926, 1905). The 18th century contained a further three events (1737, 1723, 1718) while only one extreme El Niño event of A.D. 1650 was recorded during the 16th and 17th centuries. The 20th century represents the peak of El Niño activity, when twelve events were classed as either very strong or extreme. A total of 46 very strong to extreme La Niña events were reconstructed, twelve of these classified as extreme. Four extreme La Niña events (1998, 1974, 1953, 1950) were reconstructed during the 20th century. The pre-instrumental period indicates relatively more La Niña activity with 6 (24) extreme (very strong) events compared to 4 (18) extreme (very strong) events from the El Niño reconstruction. Considerable La Niña activity is indicated during the 16th to mid 17th centuries when five extreme events are reconstructed. A trend towards increased La Niña activity over the 20th century is also evident from Table 9.

### 5.4 Event magnitude analysis results

#### 5.4.1 ENSO events since A.D. 1525

Next, changes in the relative frequency, duration and magnitude of reconstructed ENSO events were examined. The five *MQ* defined magnitude classes (outlined in Section 4.2.2) for each phase were calculated to show changes in the proportions of ENSO years per decade (per century), are displayed in Fig. 5 (Fig. 6).

A period of relative El Niño inactivity is observed from the 1670s to 1700s (upper panel of Fig. 5), including one decade (1670s) where no El Niño years were reconstructed. From the 1700s to the 1720s, events length was comparable or longer than those in the observational period but was mostly weak to moderate (see Table 9). There is a reduction in the frequency and duration of El Niño events from the 1730s to 1780s, with the exception of the extreme event noted during the 1730s.

The number of strong, very strong and extreme El Niño episodes begins increasing in the mid 19th century. Interestingly, approximately 42% of all very strong El Niño event years in the 478-year reconstruction occurs within the instrumental (post-1870)

**Table 9** El Niño and La Niña multi-proxy event lists (A.D. 1525–2002) based on the minimum quality adjusted magnitude score (MQ) associated with the three (four) proxy replication thresholds used to classify an El Niño (La Niña) event. Quality adjusted magnitude score (MQ) classes were assigned using the percentile analyses shown in Fig. 3. ‘PR’ refers to proxy ratio i.e. the number of records indicating an ENSO signal relative to total number of proxies available, ‘MS’ mean skill of the proxy subset, ‘and ‘MC’ magnitude classification. A percentile analysis of the MQ time series was used to classify MC into extreme (>90th percentile) very strong (70th–90th percentile), strong (50th–70th), moderate (50th–30th) and weak events (<30th)

El Niño year	PR	MS	MQ	MC	La Niña year	PR	MS	MQ	MC
<b>2002</b>	1/1	0.74	0.74	E	<b>2000</b>	1/2	0.73	0.37	S
<b>1997</b>	1/3	0.76	0.25	W	<b>1998</b>	3/4	0.68	0.51	E
<b>1992</b>	3/5	0.73	0.44	VS	<b>1996</b>	2/5	0.72	0.29	M
<b>1991</b>	3/5	0.70	0.42	VS	<b>1995</b>	3/6	0.72	0.33	S
					<b>1990</b>	4/7	0.69	0.39	VS
<b>1987</b>	3/6	0.73	0.37	VS	<b>1989</b>	5/7	0.69	0.49	VS
<b>1985</b>	2/7	0.78	0.22	W	<b>1988</b>	3/7	0.67	0.29	M
<b>1983</b>	6/9	0.72	0.48	E	<b>1986</b>	3/7	0.68	0.29	M
<b>1982</b>	6/10	0.78	0.46	E	<b>1985</b>	3/8	0.63	0.24	W
<b>1980</b>	4/10	0.70	0.28	M	<b>1984</b>	4/10	0.67	0.27	M
<b>1979</b>	4/11	0.79	0.29	M	<b>1975</b>	5/9	0.66	0.36	S
<b>1977</b>	3/11	0.74	0.20	W	<b>1974</b>	9/11	0.68	0.56	E
<b>1976</b>	5/11	0.71	0.32	M	<b>1973</b>	4/11	0.67	0.24	W
<b>1973</b>	3/11	0.74	0.20	W	<b>1972</b>	4/11	0.68	0.25	W
<b>1972</b>	5/11	0.76	0.35	M	<b>1971</b>	7/11	0.67	0.43	VS
					<b>1970</b>	5/11	0.65	0.30	M
<b>1969</b>	5/11	0.73	0.33	S	<b>1968</b>	4/11	0.67	0.24	W
<b>1968</b>	5/11	0.76	0.34	S	<b>1963</b>	4/11	0.68	0.25	W
<b>1967</b>	3/11	0.70	0.19	W	<b>1962</b>	4/11	0.67	0.25	W
<b>1966</b>	4/11	0.80	0.29	M	<b>1960</b>	4/11	0.67	0.25	W
<b>1965</b>	5/11	0.76	0.35	S					
<b>1964</b>	5/11	0.71	0.32	S					
<b>1959</b>	3/11	0.75	0.20	W	<b>1959</b>	4/11	0.69	0.25	W
<b>1958</b>	4/11	0.74	0.27	M	<b>1958</b>	5/11	0.66	0.30	M
<b>1957</b>	5/11	0.71	0.32	S	<b>1957</b>	4/11	0.70	0.25	W
<b>1952</b>	3/11	0.80	0.22	W	<b>1956</b>	7/11	0.68	0.43	VS
<b>1951</b>	4/11	0.79	0.29	M	<b>1955</b>	6/11	0.67	0.36	S
					<b>1953</b>	9/11	0.68	0.56	E
					<b>1951</b>	5/11	0.68	0.31	M
					<b>1950</b>	8/11	0.69	0.50	E
<b>1949</b>	3/11	0.75	0.20	W	<b>1946</b>	6/11	0.69	0.38	S
<b>1947</b>	3/11	0.71	0.19	W	<b>1945</b>	4/11	0.69	0.25	W
<b>1944</b>	5/11	0.72	0.33	S	<b>1943</b>	4/11	0.66	0.24	W
<b>1942</b>	7/11	0.72	0.46	E					
<b>1941</b>	7/11	0.76	0.48	E					
<b>1940</b>	6/11	0.72	0.39	VS					
<b>1939</b>	4/11	0.77	0.28	M	<b>1934</b>	3/11	0.69	0.25	W
<b>1938</b>	4/11	0.72	0.26	M	<b>1932</b>	4/11	0.67	0.24	W
<b>1937</b>	3/11	0.70	0.19	W					
<b>1935</b>	3/11	0.72	0.26	W					
<b>1933</b>	3/11	0.73	0.20	W					
<b>1931</b>	5/11	0.75	0.34	S					
<b>1930</b>	4/11	0.74	0.27	M					

**Table 9** (continued)

El Niño year	PR	MS	MQ	MC	La Niña year	PR	MS	MQ	MC
<b>1926</b>	8/11	0.74	0.54	E	<b>1923</b>	5/11	0.68	0.31	W
<b>1925</b>	5/11	0.78	0.35	S	<b>1922</b>	6/11	0.69	0.38	S
<b>1924</b>	3/11	0.73	0.20	W	<b>1921</b>	4/11	0.70	0.25	W
<b>1920</b>	3/11	0.82	0.22	W					
<b>1919</b>	5/11	0.75	0.34	S	<b>1918</b>	6/11	0.69	0.38	S
<b>1918</b>	5/11	0.79	0.36	VS	<b>1917</b>	7/11	0.67	0.43	VS
<b>1915</b>	6/11	0.80	0.43	VS	<b>1916</b>	6/11	0.68	0.32	S
<b>1914</b>	6/11	0.74	0.40	VS					
<b>1913</b>	6/11	0.79	0.43	VS					
<b>1912</b>	6/11	0.74	0.40	VS					
<b>1911</b>	4/11	0.79	0.29	M					
<b>1906</b>	3/11	0.73	0.20	W	<b>1910</b>	8/11	0.68	0.44	VS
<b>1905</b>	7/11	0.76	0.48	E	<b>1909</b>	6/11	0.70	0.38	VS
<b>1904</b>	3/11	0.83	0.22	W	<b>1908</b>	6/11	0.68	0.32	S
<b>1903</b>	3/11	0.70	0.19	W	<b>1907</b>	5/11	0.67	0.31	M
<b>1902</b>	6/11	0.76	0.41	VS	<b>1904</b>	5/11	0.68	0.26	W
<b>1901</b>	4/11	0.82	0.30	S					
<b>1900</b>	6/11	0.75	0.41	VS					
<b>1899</b>	4/11	0.82	0.30	S	<b>1896</b>	4/11	0.70	0.25	W
<b>1897</b>	5/11	0.77	0.30	S	<b>1894</b>	8/11	0.70	0.51	E
<b>1896</b>	4/11	0.76	0.27	M	<b>1893</b>	7/11	0.69	0.39	VS
<b>1891</b>	6/11	0.77	0.42	VS	<b>1892</b>	7/11	0.68	0.38	S
					<b>1891</b>	4/11	0.69	0.25	W
					<b>1890</b>	6/11	0.67	0.36	S
<b>1889</b>	3/11	0.77	0.21	W	<b>1887</b>	7/11	0.68	0.38	VS
<b>1888</b>	6/11	0.73	0.40	VS	<b>1886</b>	5/11	0.67	0.30	M
<b>1885</b>	5/11	0.77	0.35	S	<b>1880</b>	7/11	0.69	0.38	VS
<b>1884</b>	3/11	0.73	0.20	W					
<b>1881</b>	4/11	0.74	0.27	M					
<b>1878</b>	4/11	0.72	0.26	M	<b>1879</b>	9/11	0.69	0.51	E
<b>1877</b>	5/11	0.80	0.37	VS	<b>1878</b>	4/11	0.67	0.24	W
<b>1876</b>	3/11	0.79	0.21	W	<b>1875</b>	6/11	0.68	0.32	S
<b>1874</b>	3/11	0.73	0.20	W	<b>1874</b>	5/11	0.71	0.32	S
					<b>1873</b>	6/11	0.70	0.38	VS
					<b>1872</b>	5/11	0.69	0.31	M
					<b>1871</b>	6/11	0.72	0.39	VS
					<b>1870</b>	7/11	0.69	0.39	VS
<b>1868</b>	5/11	0.79	0.36	VS	<b>1868</b>	5/11	0.70	0.32	S
<b>1866</b>	5/11	0.79	0.36	VS	<b>1867</b>	6/11	0.69	0.38	S
<b>1865</b>	4/11	0.80	0.29	M	<b>1866</b>	5/11	0.67	0.31	M
<b>1864</b>	3/11	0.83	0.22	W	<b>1864</b>	4/11	0.71	0.26	W
<b>1860</b>	3/11	0.84	0.23	W	<b>1863</b>	7/11	0.68	0.44	VS
					<b>1862</b>	5/11	0.69	0.31	M
					<b>1861</b>	8/11	0.69	0.50	VS
					<b>1860</b>	6/11	0.70	0.38	VS
<b>1858</b>	4/11	0.73	0.27	M	<b>1857</b>	4/11	0.70	0.25	W
<b>1857</b>	4/11	0.71	0.26	M	<b>1851</b>	5/11	0.69	0.31	M
<b>1856</b>	4/11	0.74	0.27	M	<b>1850</b>	4/11	0.67	0.24	W
<b>1853</b>	5/11	0.82	0.37	VS					
<b>1852</b>	3/11	0.76	0.21	W					

**Table 9** (continued)

El Niño year	PR	MS	MQ	MC	La Niña year	PR	MS	MQ	MC
<b>1848</b>	3/11	0.74	0.20	W	<b>1849</b>	5/11	0.68	0.31	M
<b>1847</b>	3/11	0.74	0.20	W	<b>1848</b>	4/11	0.69	0.25	W
<b>1846</b>	3/11	0.75	0.20	W	<b>1847</b>	6/11	0.69	0.38	S
<b>1845</b>	6/11	0.75	0.41	VS	<b>1843</b>	5/11	0.70	0.26	W
<b>1844</b>	4/11	0.79	0.29	M	<b>1841</b>	4/11	0.68	0.25	W
					<b>1840</b>	4/11	0.70	0.25	W
<b>1838</b>	3/11	0.80	0.22	W	–				
<b>1837</b>	4/11	0.82	0.30	S					
<b>1833</b>	5/11	0.78	0.35	S					
<b>1832</b>	3/11	0.80	0.22	W					
<b>1829</b>	3/11	0.74	0.20	W	<b>1825</b>	5/11	0.68	0.31	M
<b>1824</b>	4/11	0.79	0.29	M	<b>1823</b>	4/10	0.71	0.28	M
					<b>1820</b>	5/10	0.70	0.35	S
<b>1817</b>	4/10	0.75	0.30	S	<b>1819</b>	5/10	0.69	0.35	S
<b>1816</b>	3/10	0.78	0.23	W	<b>1813</b>	4/10	0.71	0.29	M
<b>1815</b>	3/10	0.77	0.23	W	<b>1811</b>	5/10	0.69	0.34	S
<b>1814</b>	3/10	0.78	0.23	W	<b>1810</b>	5/10	0.69	0.34	S
<b>1812</b>	4/10	0.82	0.33	S					
<b>1807</b>	4/10	0.75	0.30	S	<b>1809</b>	5/10	0.72	0.36	S
<b>1806</b>	5/10	0.79	0.40	VS	<b>1808</b>	7/10	0.69	0.48	VS
<b>1804</b>	3/10	0.78	0.23	W	<b>1805</b>	7/20	0.69	0.49	VS
<b>1803</b>	4/10	0.82	0.33	S	<b>1802</b>	7/10	0.68	0.48	VS
					<b>1801</b>	6/10	0.69	0.42	VS
<b>1799</b>	5/11	0.76	0.34	S	<b>1798</b>	4/11	0.70	0.25	W
<b>1798</b>	3/11	0.74	0.20	W	<b>1797</b>	5/11	0.69	0.31	M
<b>1794</b>	4/11	0.74	0.27	M	<b>1795</b>	4/11	0.69	0.25	W
<b>1793</b>	4/11	0.74	0.27	M	<b>1790</b>	5/11	0.70	0.32	S
<b>1792</b>	3/11	0.72	0.20	W					
<b>1791</b>	6/11	0.78	0.42	VS					
<b>1784</b>	3/11	0.72	0.20	W	<b>1789</b>	4/11	0.71	0.26	W
<b>1783</b>	4/11	0.80	0.29	M	<b>1788</b>	6/11	0.70	0.38	VS
<b>1782</b>	3/11	0.80	0.22	W	<b>1787</b>	6/11	0.69	0.37	S
					<b>1786</b>	5/11	0.70	0.32	S
					<b>1785</b>	4/11	0.72	0.26	W
					<b>1782</b>	4/11	0.70	0.25	W
					<b>1780</b>	5/11	0.71	0.32	S
<b>1777</b>	3/11	0.76	0.21	W	<b>1779</b>	5/11	0.70	0.32	S
<b>1770</b>	5/11	0.79	0.36	VS	<b>1778</b>	4/11	0.70	0.26	W
					<b>1776</b>	4/11	0.72	0.26	W
					<b>1773</b>	4/11	0.71	0.26	W
					<b>1772</b>	5/11	0.69	0.31	M
<b>1769</b>	4/11	0.79	0.29	M	<b>1765</b>	6/11	0.69	0.37	S
<b>1768</b>	3/11	0.75	0.20	W	<b>1763</b>	5/11	0.70	0.32	S
<b>1766</b>	3/11	0.76	0.21	W	<b>1761</b>	5/11	0.69	0.32	M
<b>1754</b>	3/11	0.75	0.20	W	<b>1758</b>	4/11	0.68	0.25	W
					<b>1757</b>	6/11	0.69	0.37	M
					<b>1756</b>	5/11	0.69	0.31	M
					<b>1755</b>	5/11	0.70	0.32	S
					<b>1754</b>	5/11	0.69	0.31	M
					<b>1753</b>	6/11	0.69	0.38	S

**Table 9** (continued)

El Niño year	PR	MS	MQ	MC	La Niña year	PR	MS	MQ	MC
					<b>1752</b>	7/11	0.69	0.44	VS
					<b>1751</b>	5/11	0.69	0.31	M
					<b>1750</b>	5/11	0.70	0.32	S
<b>1748</b>	4/11	0.77	0.28	M	<b>1748</b>	4/11	0.70	0.26	W
<b>1747</b>	4/11	0.81	0.29	M	<b>1747</b>	4/11	0.72	0.26	W
<b>1746</b>	3/11	0.83	0.22	W	<b>1745</b>	5/11	0.71	0.32	S
<b>1744</b>	3/11	0.83	0.22	W	<b>1743</b>	6/11	0.70	0.38	VS
					<b>1742</b>	8/11	0.70	0.51	E
					<b>1741</b>	5/11	0.70	0.32	S
					<b>1740</b>	7/11	0.70	0.45	VS
<b>1738</b>	3/11	0.71	0.19	W	<b>1739</b>	6/11	0.70	0.38	VS
<b>1737</b>	7/11	0.79	0.50	E	<b>1736</b>	4/11	0.72	0.26	W
<b>1734</b>	3/11	0.78	0.21	W	<b>1735</b>	4/11	0.72	0.26	W
					<b>1733</b>	6/11	0.70	0.38	VS
					<b>1732</b>	5/11	0.69	0.31	M
					<b>1731</b>	5/11	0.68	0.31	M
					<b>1730</b>	4/11	0.70	0.25	W
<b>1729</b>	3/11	0.73	0.20	W	<b>1725</b>	4/10	0.68	0.27	M
<b>1728</b>	5/11	0.78	0.35	S	<b>1724</b>	4/10	0.69	0.28	M
<b>1726</b>	3/10	0.75	0.23	W					
<b>1724</b>	3/10	0.77	0.23	W					
<b>1723</b>	6/10	0.76	0.46	E					
<b>1722</b>	4/10	0.73	0.29	M					
<b>1721</b>	3/10	0.76	0.23	W					
<b>1720</b>	3/10	0.77	0.23	W					
<b>1719</b>	4/9	0.75	0.33	S	<b>1716</b>	5/10	0.70	0.35	S
<b>1718</b>	5/9	0.79	0.44	E	<b>1715</b>	5/10	0.69	0.35	S
<b>1714</b>	3/10	0.74	0.22	W					
<b>1713</b>	4/10	0.74	0.30	M					
<b>1712</b>	3/10	0.76	0.23	W					
<b>1710</b>	3/10	0.75	0.23	W	<b>1709</b>	4/10	0.69	0.28	M
<b>1709</b>	3/10	0.80	0.24	W	<b>1708</b>	5/10	0.68	0.34	S
<b>1707</b>	3/10	0.78	0.23	W	<b>1702</b>	4/10	0.69	0.28	M
<b>1700</b>	3/9	0.75	0.25	W	<b>1701</b>	4/10	0.70	0.28	M
<b>1695</b>	3/9	0.73	0.24	W	<b>1696</b>	5/9	0.71	0.39	VS
<b>1694</b>	4/9	0.72	0.32	S	<b>1690</b>	4/9	0.69	0.31	M
<b>1692</b>	3/9	0.73	0.24	W					
<b>1687</b>	5/9	0.79	0.43	VS	<b>1686</b>	4/9	0.70	0.31	M
<b>1684</b>	3/9	0.75	0.25	W	<b>1685</b>	4/9	0.72	0.32	S
					<b>1678</b>	4/9	0.70	0.31	M
					<b>1676</b>	4/9	0.72	0.32	S
					<b>1675</b>	4/9	0.69	0.30	M
					<b>1668</b>	4/9	0.69	0.31	M
<b>1669</b>	3/9	0.75	0.25	W	<b>1663</b>	5/9	0.69	0.39	VS
<b>1665</b>	3/9	0.75	0.25	W					
<b>1661</b>	4/9	0.79	0.35	S					
<b>1660</b>	5/9	0.79	0.44	VS					
<b>1659</b>	3/9	0.84	0.28	M	<b>1658</b>	4/9	0.70	0.31	M
<b>1652</b>	3/9	0.75	0.25	W	<b>1654</b>	5/8	0.71	0.44	VS
<b>1651</b>	3/9	0.75	0.25	W					

**Table 9** (continued)

<b>El Niño year</b>	<b>PR</b>	<b>MS</b>	<b>MQ</b>	<b>MC</b>	<b>La Niña year</b>	<b>PR</b>	<b>MS</b>	<b>MQ</b>	<b>MC</b>
<b>1650</b>	6/9	0.79	0.52	E					
<b>1648</b>	3/9	0.82	0.27	M	<b>1649</b>	3/8	0.70	0.26	W
<b>1646</b>	3/9	0.75	0.25	W	<b>1648</b>	3/8	0.72	0.27	W
<b>1642</b>	3/9	0.74	0.24	W	<b>1645</b>	6/8	0.69	0.52	E
<b>1641</b>	3/9	0.75	0.25	W	<b>1644</b>	4/8	0.69	0.34	S
					<b>1642</b>	4/8	0.70	0.35	S
					<b>1641</b>	5/8	0.70	0.44	VS
<b>1639</b>	3/9	0.72	0.24	W	<b>1639</b>	3/8	0.71	0.27	M
<b>1638</b>	3/9	0.77	0.26	W	<b>1638</b>	3/8	0.72	0.27	M
<b>1635</b>	4/9	0.72	0.32	M	<b>1637</b>	4/8	0.71	0.35	S
<b>1630</b>	3/9	0.83	0.28	M	<b>1635</b>	3/8	0.70	0.27	W
					<b>1632</b>	7/8	0.69	0.61	E
					<b>1631</b>	5/8	0.70	0.44	VS
					<b>1630</b>	4/8	0.68	0.34	S
<b>1621</b>	3/9	0.76	0.25	W	<b>1629</b>	4/8	0.69	0.35	S
<b>1620</b>	3/9	0.73	0.24	W	<b>1628</b>	3/8	0.69	0.26	W
					<b>1627</b>	3/8	0.69	0.26	W
					<b>1626</b>	5/8	0.69	0.43	VS
					<b>1625</b>	3/8	0.72	0.27	M
					<b>1624</b>	5/8	0.71	0.45	VS
					<b>1623</b>	5/8	0.71	0.44	VS
					<b>1622</b>	4/8	0.69	0.34	S
<b>1619</b>	4/9	0.77	0.34	S	<b>1612</b>	4/9	0.70	0.31	M
<b>1618</b>	5/9	0.79	0.44	VS	<b>1611</b>	4/9	0.70	0.35	S
<b>1614</b>	3/10	0.83	0.25	W					
<b>1609</b>	3/9	0.75	0.25	W	<b>1605</b>	3/7	0.69	0.30	M
<b>1608</b>	5/9	0.76	0.42	VS	<b>1604</b>	3/7	0.69	0.30	M
<b>1607</b>	5/9	0.73	0.41	VS	<b>1603</b>	3/7	0.68	0.29	M
<b>1601</b>	3/9	0.78	0.26	M	<b>1602</b>	3/7	0.68	0.29	M
					<b>1601</b>	3/7	0.70	0.30	M
					<b>1600</b>	4/7	0.70	0.40	VS
<b>1597</b>	3/9	0.80	0.27	M	<b>1597</b>	3/7	0.71	0.30	M
<b>1596</b>	5/9	0.77	0.34	S	<b>1593</b>	3/7	0.72	0.41	VS
<b>1594</b>	4/9	0.77	0.34	S	<b>1592</b>	4/7	0.71	0.40	VS
<b>1591</b>	4/9	0.74	0.33	S	<b>1590</b>	3/7	0.72	0.31	M
<b>1585</b>	4/8	0.74	0.37	VS	<b>1584</b>	4/6	0.71	0.47	VS
<b>1584</b>	3/8	0.70	0.26	M	<b>1583</b>	3/6	0.71	0.36	S
<b>1583</b>	3/8	0.72	0.27	M	<b>1581</b>	3/6	0.69	0.35	S
					<b>1580</b>	3/6	0.69	0.35	S
<b>1574</b>	4/8	0.74	0.37	VS	<b>1579</b>	3/6	0.71	0.36	S
					<b>1578</b>	3/6	0.71	0.36	S
					<b>1577</b>	3/6	0.70	0.35	S
					<b>1576</b>	3/6	0.71	0.36	S
					<b>1573</b>	4/6	0.70	0.58	E
					<b>1572</b>	5/6	0.70	0.58	E
					<b>1571</b>	3/6	0.69	0.35	S
<b>1567</b>	3/8	0.78	0.28	M	<b>1566</b>	3/6	0.70	0.35	S
<b>1565</b>	4/8	0.75	0.38	VS	<b>1561</b>	3/6	0.71	0.35	S
<b>1563</b>	3/8	0.75	0.28	M	<b>1560</b>	4/6	0.70	0.23	VS
<b>1559</b>	4/8	0.75	0.38	VS					
<b>1558</b>	3/8	0.78	0.29	M					

**Table 9** (continued)

El Niño year	PR	MS	MQ	MC	La Niña year	PR	MS	MQ	MC
<b>1556</b>	4/8	0.75	0.40	VS					
<b>1554</b>	4/8	0.79	0.30	S					
<b>1544</b>	4/8	0.75	0.38	VS	<b>1549</b>	3/6	0.69	0.35	S
<b>1540</b>	3/8	0.83	0.31	S	<b>1548</b>	3/6	0.71	0.47	VS
					<b>1546</b>	3/6	0.70	0.35	S
					<b>1544</b>	3/6	0.70	0.35	S
					<b>1542</b>	3/6	0.72	0.36	S
					<b>1541</b>	3/6	0.71	0.36	VS
					<b>1540</b>	3/6	0.69	0.34	S
<b>1539</b>	3/8	0.74	0.28	M	<b>1538</b>	3/6	0.72	0.36	S
					<b>1535</b>	3/6	0.70	0.35	S
					<b>1533</b>	6/6	0.70	0.70	E
					<b>1532</b>	4/6	0.70	0.47	VS
					<b>1531</b>	4/6	0.70	0.47	VS
<b>1527</b>	3/8	0.73	0.27	M	<b>1528</b>	5/6	0.70	0.58	E
<b>1526</b>	4/8	0.72	0.36	VS					
<b>1525</b>	4/8	0.72	0.36	VS					

period. The highest proportion of reconstructed El Niño years outside of the 18th century is reconstructed in the 1900s and 1910s when 70% of each of these decades appear to have been characterised by persistent El Niño conditions; 57% and 86% of which fell within strong to extreme magnitude categories, respectively. The 1940s and 1980s, have the highest proportion of extreme event years in the reconstruction, where at least 50% of the El Niño years were extreme. Overall, 55% of extreme El Niño event years reconstructed since A.D. 1525 occur within the 20th century (1900s, 1920s, 1940s, 1980s).

The 16th to mid 17th centuries stands out as the most sustained period of La Niña activity, with the exception of the 1550s when no La Niñas were reconstructed (Fig. 5). From the 1520s to 1660s thirteen (five) very strong (extreme) La Niña events are observed. Notably, from the 1650s to the 1720s, there is a general reduction of La Niña activity, with three decades (1650s, 1660s, 1690s) displaying extreme or strong event years, suggesting a low frequency but relatively high magnitude of events during this period. From the 1720s, a period of increased La Niña activity is seen through to the beginning of the 20th century. The majority of these event years are, however, weak to moderate. The maximum number of La Niña years in the entire record occurs in the 1750s when La Niña dominated 90% of the decade.

A period of notable La Niña activity was reached during the 19th century when 53% of the century was characterised by La Niña conditions (Fig. 6). The 1860s and 1870s are the only two decades that to consecutively register La Niña conditions 80% of the time. Similarly, six consecutive decades of very strong to extreme La Niña episodes (1860s–1910s) are noted. The late 19th century to the end of 20th century is characterised by an increase in the proportion of strong, very strong and extreme La Niña events (1870s, 1890s, 1950s, 1970s, 1990s); a trend also observed in the El Niño reconstruction. Overall, 26% of the 19th and 30% of the 20th centuries were classed as very strong to extreme La Niña years (Fig. 6).

Between 1920s and 1960s there is an overall reduction in the frequency of La Niña events, corresponding with a period of less frequent, but extreme El Niño events. The

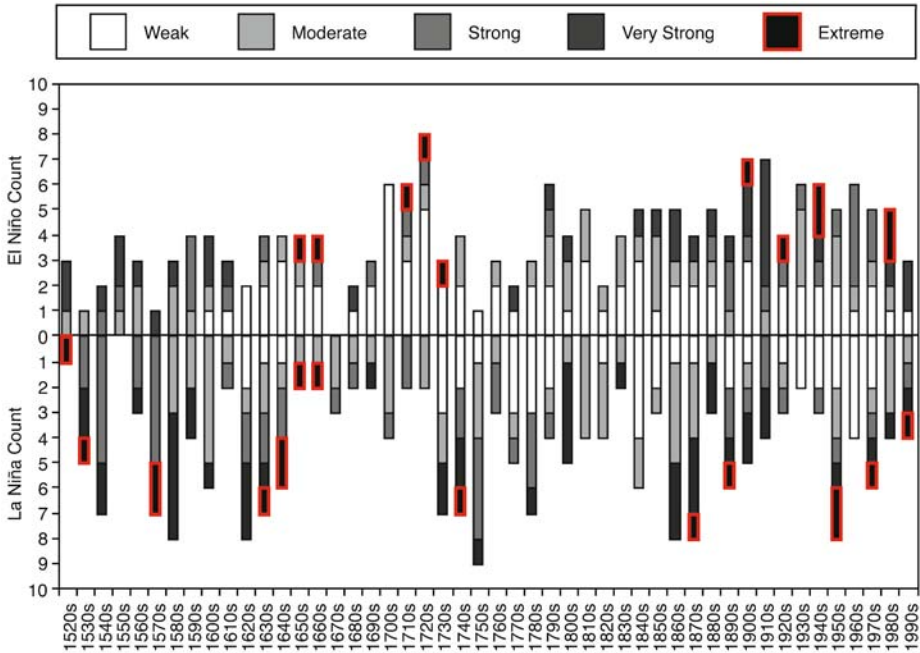


**Fig. 5** Decadal trends in reconstructed El Niño and La Niña event magnitude characteristics, A.D. 1525–2000. Five percentile classes of the MQ time series were used to classify ENSO magnitude into extreme (>90th percentile) very strong (70th–90th percentile), strong (50th–70th), moderate (50th–30th) and weak events (<30th)

notable exception is the 1950s, when very strong or extreme event years are seen. Following weak La Niña conditions in the 1960s (a period dominated by strong El Niño activity), the 1970s to 1990s shows three consecutive decades when very strong to extreme events La Niña years were observed.

Overall there has been a general increase in the number of ENSO years reconstructed from this multi-proxy study. For example, during the 1500s, a total of 21 El Niño years were reconstructed compared to over 54 during the 20th century. Peak La Niña frequency is observed during the 18th and 19th centuries when approximately 50 La Niña years were reconstructed, falling to 43 by the 20th century. Strikingly, 43% of all extreme ENSO events reconstructed since A.D. 1525 occur in the 20th century.

*5.4.2 Protracted ENSO episodes*

Following Allan and D’Arrigo (1999), a protracted event is defined here as persisting for three years or more. To investigate the frequency of protracted ENSO episodes through time, all events listed in Table 9 exceeding three years were extracted (Table 10). There are a total of 24 (26) protracted El Niño (La Niña) events, 28% of which occurred in the 20th century. The longest La Niña spanned 11 years (A.D. 1622–1632), and the longest El Niño events reconstructed lasted seven years (A.D. 1900–1906 and A.D. 1718–1724).

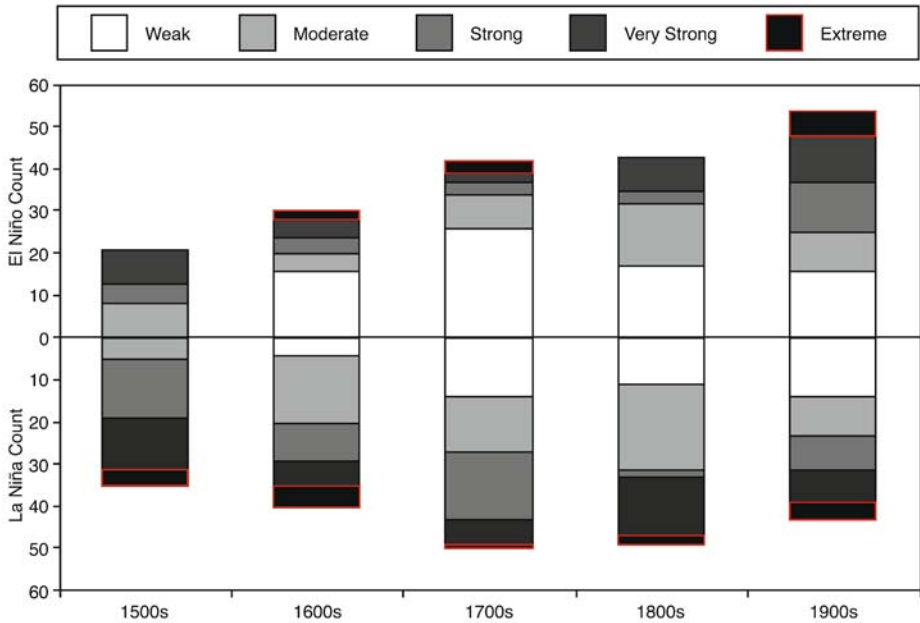


**Fig. 6** Centennial trends in ENSO episodes reconstructed for A.D. 1525–2002. Five percentile classes of the MQ time series were used to classify ENSO magnitude into extreme (>90th percentile) very strong (70th–90th percentile), strong (50th–70th), moderate (50th–30th) and weak events (<30th)

Interestingly, more events are reconstructed from our reconstruction than the 23 (17) protracted El Niño (La Niña) events identified between A.D. 1706–1977 by Allan and D’Arrigo (1999). This may reflect the shorter length of the time series, decoupled and lead/lag signatures maintained in the calibration process, or indeed, over-reconstruction. Nevertheless, there is good agreement of the timing of the events shared by Table 10 and Allan and D’Arrigo (1999) in both observational and pre-instrumental times. The discrepancies, however, may suggest true differences between SOI event signatures compared to the combined ocean–atmosphere ENSO signals captured by the CEI.

## 6 Discussion

To calibrate single proxy records to instrumental ENSO conditions, the optimisation technique used (see Fig. 2) was essentially arbitrary. Maximising event capture at the single proxy level was desired as false positives are likely to be ‘lost’ from the larger multi-proxy environment as the likelihood of false positives occurring simultaneously in many locations is expected to be low. Results from this study show an asymmetry in ENSO phase-sensitivity of palaeoclimate records. Accordingly we recommend that El Niño and La Niña sensitive proxies be separated when reconstructing individual ENSO events.

**Table 10** Protracted CEI ENSO events reconstructed since A.D. 1525

<i>Reconstructed Protracted events</i>	<i>Duration (Years)</i>	<i>Reconstructed Protracted events</i>	<i>Duration (Years)</i>
<b><i>El Niños</i></b>			
1964–1969	6	1791–1794	4
1957–1959	3	1782–1784	3
1937–1942	6	1768–1771	4
1924–1926	3	1746–1748	3
1918–1920	3	1718–1724	7
1911–1915	5	1712–1714	3
1900–1906	7	1659–1661	3
1876–1878	3	1650–1652	3
1864–1866	3	1618–1621	4
1856–1858	3	1607–1609	3
1844–1848	5	1585–1583	3
1814–1817	4	1525–1527	3
		<b>Total</b>	24
<b><i>La Niñas</i></b>			
1988–1990	3	1808–1811	4
1984–1986	3	1785–1790	6
1970–1975	6	1778–1780	3
1955–1960	6	1750–1758	9
1921–1923	3	1739–1743	5
1916–1918	3	1730–1733	4
1907–1910	4	1637–1639	3
1890–1894	5	1622–1632	11
1878–1880	3	1600–1605	6
1870–1875	6	1576–1581	6
1866–1868	3	1571–1573	3
1860–1864	5	1540–1542	3
1847–1851	5	1531–1533	3
		<b>Total</b>	26

Following Allan and D'Arrigo (1999), a protracted event is defined as persisting for three years or more

The lower confidence levels noted for the La Niña phase reconstruction may be related to the relatively lower number of very sensitive La Niña records (Table 3). To compensate for the fewer La Niña proxies available for ENSO reconstruction, three slightly less skilful La Niña proxies (D'Arrigo Teak (0.6), Great Barrier Reef (0.65) and New Caledonia (0.64)) were used to match the number of records used for the El Niño phase reconstruction (12). This could explain the higher number of false positive cases seen in the La Niña reconstruction (Table 5).

Interestingly, the tree-ring records appear to have stronger ENSO sensitivity than the other records used in this study. For example, the Mexican Douglas Fir and the Berlage Teak tree-ring records are in the top five of the most ENSO sensitive proxies (Table 3), highlighting their importance in reconstructive work. This may reflect the exact dating of tree-ring chronologies that results from rigorous replication inherent to cross-dating and chronology development. Internal replication helps enhance the common climate signal present in individual samples and reduce signal noise.

For the purpose of this study, the dating of coral records was sourced from the primary literature describing the data. No attempt was made to adjust age models provided by the scientists who contributed the proxy data. It is possible that the weaker sensitivities found in coral sequences is a consequence of dating issues

and/or non-stationary trends reported elsewhere (Gagan et al. 2000; Hendy et al. 2003; Linsley et al. 2004; Lough 2004). Until improved replication for regional coral chronologies becomes commonplace (e.g. Hendy et al. 2003; Lough 2007), perhaps more emphasis should be placed on the more exactly dated tree-ring records for non-equally weighted approaches to ENSO reconstruction. It is recognised that the results presented here may contain dating errors and will only be improved as more reconstructions of past ENSO episodes become available. An exhaustive analysis of such factors, however, was beyond the scope of the analysis reported here.

The high overall proxy performance observed for the Quelccaya ice-core record (Table 3) suggests dating and/or stationarity issues are not as problematic as noted for coral. These results support the favourable assessment of the Quelccaya record used by Bradley (1996). This suggests that other high quality tropical ice-cores should be examined for any ENSO-sensitivity and incorporated into future multi-proxy analyses (Thompson 2000; Thompson et al. 2000, 2002). The high performance noted for the Quinn and Indian documentary records may reflect their listing of fewer, discrete events rather than being a continuous time series, which probably accounts for the low false positive cases listed in Table 3.

To address the lack of precisely dated, equatorial proxies and a loss of proxy records through time, no geographical equal weighting was applied to records from core/teleconnection and east/west Pacific regions. Ideally, climatically sensitive records from the equatorial Pacific centres-of-action of ENSO would be used to reconstruct core characteristics of ENSO, and all remaining annual resolution proxies could then be used to map the spatial patterns of tropical and extra-tropical teleconnections signals associated with each reconstructed ENSO event (Stahle et al. 1998). A lack of proxy data from the tropics currently precludes this.

Since ENSO teleconnection patterns can fluctuate considerably, it is worth remembering that reconstructions based on more peripheral extra-tropical sites may not be as stable through time. Nevertheless, comparisons between the full and the smaller A.D. 1525 subset reconstructions show an internal robustness of the multi-proxy chronology analysed here. Adjusting for overall replication and proxy skill in the MQ time series produces a more robust measure for assessing reconstruction reliability rather than assessment based on mean skill (MS) of a proxy subset alone. This suggests that quality may be more important than the overall quantity (replication) of proxy records used for ENSO reconstruction. Interestingly, the subsets of records continuously present back to A.D. 1525 are based on proxies from extra-tropical teleconnection regions (e.g. New Zealand, Mexico and the USA) rather than core equatorial Pacific sites. This suggests that in lieu of well-replicated, exactly-dated equatorial proxies, robust chronologies from key teleconnection areas remain our strongest evidence of past ENSO behaviour (Stahle et al. 1998).

Verification consistent with the approaches of Whetton and Rutherford (1994) and Allan and D'Arrigo (1999) revealed that our reconstructions compared well with the two primary long-term El Niño (La Niña) event lists of QO00 and WR94. This study provides further replication of the events reported by previous research and significantly introduces the first substantial La Niña event list for the pre-observational period compiled to date. Although there is more uncertainty associated with the reconstruction due to fewer La Niña sensitive proxies, considerable skill is still achieved (Section 5.2).

Generally, the duration of La Niña events in the reconstructions were found to be greater than their El Niño counterparts. Table 10 lists seven protracted La Niña events lasting six years or more, including one eleven-year episode (A.D. 1622–1632). This compares to a maximum duration of 7 years for an El Niño event (A.D. 1718–1724 and 1900–1906). If the trends reported here are considered to be reliable, it may signify important differences in the past nature of El Niño and La Niña events and an important contribution to a noticeable gap in the Inter-governmental Panel on Climate Change's (IPCC) El Niño-focused assessment of past ENSO behaviour (Jansen et al. 2007).

Our results are in agreement with the conclusion of Allan and D'Arrigo (1999) that 'persistent' ENSO event sequences have occurred prior to the observational period, and that the 1990–1995 El Niño event recorded by the SOI (not seen in our coupled atmosphere–ocean based reconstructions) is not unprecedented from the context of the past 478 years. It is noteworthy that 28% of all protracted ENSO events reconstructed here occur in 20th century, a widely recognised period of heightened ENSO activity (Trenberth et al. 2007). Allan (2000) suggested that the existence of protracted ENSO events may be due to the phasing of high frequency (quasi-biennial)  $\sim 2$  year activity with the 'classical' 3–7 year (lower frequency) ENSO variability. The investigation of such characteristics would require spectral analysis not possible using the discrete ENSO event reconstruction techniques employed here. Spectral characteristics are best analysed using PCA/EOF-based reconstructions of ENSO indices, and are the subject of a forthcoming paper (Braganza et al. 2008).

Quinn and Neal (1992) identified periods of apparently anomalous long-term El Niño behaviour from their South American reconstruction. These near-decadal or longer periods include A.D. 1539–1578, 1600–1624, 1701–1728, 1792–1802, 1812–1832, 1864–1891, 1897–1919, 1925–1932 and 1976–1987. Jones and Bradley (1992) recommended that these intervals should be the focus of future research to determine the larger scale significance of periods with above or below average ENSO frequency. Accordingly, these intervals were examined from our reconstruction to reveal similar periods of extended El Niño activity (1525–1565, 1596–1635, 1712–1738, 1768–1807, 1812–1853, 1864–1891, 1896–1944, 1957–1976 and 1982–2002) when many high magnitude events are recorded.

ENSO behaviour has fluctuated significantly since A.D. 1525. A notable period of reduced ENSO activity was identified between A.D. 1650–1780 when ENSO events were largely weak to moderate. This is coincident with the timing of the broadly defined Little Ice Age ( $\sim$ A.D. 1550–1850) (Lamb 1982) and more specifically, the Maunder Minimum period of low solar variability ( $\sim$ A.D. 1645–1715) (Eddy 1977; Reid 1997). This period of overall quiescence is, however, punctuated by a number of very strong to extreme La Niñas particularly in the 1620s to 1640s. This is broadly consistent with intense 17th century ENSO activity reported by Cobb et al. (2003).

Whetton and Rutherford (1994) tentatively concluded that ENSO teleconnections were less active during the broadly defined Little Ice Age (or pre-20th century cold period) compared to the middle of the 19th century. They were, however, not confident that the data used in the early part of the record was sufficiently reliable. They stated, 'until we have better evidence to the contrary, [El Niño and La Niña] events may be assumed to have occurred over recent centuries at something like the frequency and intensity observed over the instrumental period' (Whetton and Rutherford 1994:249). Having presented further evidence for the pre-20th century

period, this study suggests that ENSO has displayed considerably variability over the past five centuries. A prominent decrease (increase) in ENSO activity coincides with the duration (termination) of the LIA. This result is consistent with D'Arrigo et al. (2005) who present evidence from North American tree-rings over the past six centuries.

The height of extreme La Niña activity is seen from the 16th to mid 17th centuries, when 56% of all the extreme La Niña years reconstructed occurs. These trends may reflect a loss of records (sample depth) for the early part of the reconstruction when only six La Niña sensitive records (compared to eight El Niño proxies) are present. Since there is a reduction in the relative proportions of responsive proxies to available sample depth, there may be a slight amplification of the magnitude of La Niña presented here. Nonetheless, if the results reported in this study are representative of real trends in La Niña event magnitude, it may suggest that periods of more extreme La Niña events than have currently been witnessed could be expected in the future (Timmermann et al. 1999).

Interestingly, the 20th century contains over 43% of all the reconstructed extreme ENSO events seen in Table 9. The post-1940 period alone accounts for 30% of these extreme climate events. Despite efforts to adjust for proxy skill, it is acknowledged that event magnitude may be relatively underestimated at the tail ends of the time series due to the inevitable reduction in sample depth. There are, however, still eight (six) El Niño (La Niña) proxies present in the reconstruction back to A.D. 1525. The sub-sample analysis presented in Section 5.2.2 also suggests the overall reliability of the reconstructions even with a loss of records through time. The lack of proxy coverage seen late in the observational period (largely post-1990) is not as problematic as higher quality instrumental data is available for comparison with the long-term reconstructions. Of the extreme events noted by Gergis and Fowler (2005) in the instrumental CEI, 50% of all extreme ENSO events are observed post-1970, suggesting real climatic trends in the reconstruction rather than an artefact of the methodology employed here.

Analysis of the multi-proxy reconstruction revealed considerable ENSO variability over the past five centuries. Our results are consistent with the conclusions of D'Arrigo et al. (2005) concerning solar/temperature related modification of ENSO behaviour. Periods of inactivity were identified throughout the record; most notably, during the 1600s ENSO appears to have weakened, coincident with the height of the commonly defined Little Ice Age (~A.D. 1550–1850) and Maunder Minimum (~A.D. 1645–1715) epochs. Hendy et al.'s (2002) coral Sr/Ca SST reconstruction shows northern Australian SSTs 0.2° to 0.3°C cooler than the long-term average between 1565 and 1700. This corresponds to enhanced La Niña activity in our reconstruction (1520s to 1660s) and a period of relative El Niño quiescence from the 1600s to 1780s.

Hendy et al. (2002) also note a conspicuous period from their Sr/Ca SST reconstruction from the 1700s to the 1870s show a consistent warming comparable to the SST warmth of the early 1980s. A Pacific coral Sr/Ca SST reconstruction from Rarotonga (Linsley et al. 2000) also shows SSTs for the 18th and 19th centuries that are as warm as, or warmer than, the 20th century. Interestingly, this period corresponds to a pronounced period of La Niña activity (see Table 9). Above-average SSTs persist through most of the 18th and 19th centuries, a period notable La Niña activity in our reconstruction, before cooling to a minimum in the early

20th century (a period of high El Niño activity). From this cold interval, Hendy et al.'s (2002) SST anomaly reconstructions captures 20th century warming. This corresponds to a marked increase in both ENSO phase extremes (with a notable El Niño bias) in the reconstructions presented here.

## 7 Conclusion

In this study, a number of proxy ENSO records (tree-ring, coral, ice-core and documentary) were examined to isolate ENSO signals associated with both phases of the phenomenon. By using a variety of regional records, it is possible to capture more of the spatial variability of ENSO more likely to be representative of large-scale ocean–atmosphere processes than is possible from single proxy analysis. Regional ENSO event signatures were compared, revealing large-scale trends in the frequency, magnitude and duration of pre-instrumental ENSO. Using novel applications of percentile analysis, a number of threshold dependent ENSO reconstructions allowed late 20th century ENSO variability to be assessed from a multi-centennial perspective with various degrees of certainty.

Clearly, multi-proxy ENSO reconstruction is still in its infancy. Abundant potential remains to characterise teleconnection patterns, low frequency changes, propagation signatures and non-stationarities of large-scale ENSO behaviour (Gergis et al. 2006). It is well recognised that there is a need for high-quality proxies from key ENSO-affected regions, particularly from the western Pacific (Hendy et al. 2003; Mc Donald et al. 2004; Boswijk et al. 2006; D'Arrigo et al. 2006; Gergis et al. 2006; Wilson et al. 2006). It is essential that existing records from these regions be further developed and/or reviewed for their ENSO-sensitivity to allow regional dynamics of the western Pacific to be resolved (D'Arrigo et al. 2006; Wilson et al. 2006).

To date, there have been limited attempts to develop chronologies of individual ENSO events for the pre-observational period using palaeoclimatic records (Quinn and Neal 1992; Whetton and Rutherford 1994; Whetton et al. 1996; Allan and D'Arrigo 1999; Ortlieb 2000; Gergis et al. 2006). Using a variety of regional ENSO signals spanning the both the east and west Pacific an extensive 478-year chronology of ENSO events was developed back to AD 1525. For the first time, there was a considerable improvement in proxy representation from western Pacific locations, allowing signals from both key ENSO 'centres-of-action' to be considered. This allowed the large-scale (rather than regional) trends in the frequency, magnitude and duration of pre-instrumental ENSO over the past five centuries. Methods for the quantification of event magnitude and reconstruction uncertainty were also provided for both ENSO phases. Significantly, the most comprehensive La Niña event chronology compiled to date is presented for the AD 1525–2002 period.

The chronology presented here expands upon the discrete ENSO event records provided by previous researchers (e.g. Quinn and Neal 1992; Ortlieb 2000 and Whetton and Rutherford 1994). Our record provides an alternative to the Quinn records commonly used by palaeoclimatologists as 'reference years' for studying past ENSO events (Stahle et al. 1998; Rodbell et al. 1999; Mann et al. 2000; Gergis 2006). Importantly, this annual record of ENSO events can now be used as an

independent means of verifying model simulations and continuous proxy reconstructions of ENSO indices (Stahle et al. 1998; Mann et al. 2000; D'Arrigo et al. 2005) and a chronological control for archaeologists and social scientists studying human responses to past climate events (Bouma et al. 1997; Grove and Chappell 2000; Kuhnel and Coates 2000; Haberle et al. 2001; Kovats et al. 2003; Goddard and Dilley 2005; Patz et al. 2005).

Discrete ENSO event reconstruction techniques differ considerably from the more common approach of using statistical techniques to extract the dominant modes of co-variability from palaeo-networks (Gergis et al. 2006). These approaches are most often some form of empirical orthogonal function (EOF) or principal component analysis (PCA) techniques (Von Storch and Zwiers 1999; Jolliffe 2002). Significantly, none of the ENSO indices reconstructed to date (Stahle et al. 1998; Mann et al. 2000; D'Arrigo et al. 2005) are able to completely reproduce the variance exhibited by the instrumental record. This may reflect both the truncation of variance due to regression-type approaches to generating transfer functions as well as inherent limitations in the ability of palaeoclimatic proxies to fully resolve the magnitude of associated climate variability (Gergis et al. 2006).

This reinforces the fact that different ENSO reconstruction techniques have important biases and limitations to consider (Gergis et al. 2006). If information is sought on the nature of individual ENSO episodes that influence society on inter-annual time scales (e.g. Hennessy et al. 2007), then event-based percentile techniques may be more appropriate than EOF/PCA reconstructions of ENSO indices, as important information on event magnitude may be lost. It is, however, important to bear in mind that trends inferred from an essentially binary approach to ENSO event reconstruction largely removes the ability to examine ENSO as a continuum of conditions in the ocean–atmosphere system. Such trends are better characterised using continuous PCA/EOF-based reconstructions of ENSO indices and are the subject of a forthcoming paper (Braganza et al. 2008) and future work. It is acknowledged that complementary research into differences in eastern/western Pacific regional signals and event evolution characteristics is warranted, however, this was beyond the scope of this study aimed at presenting an initial 'global chronology' of both ENSO phase events.

Despite their limitations, reconstructions of past climate are unique in their ability to provide a long-term context for evaluating 20th century climate change. The unusual nature of late 20th century ENSO is evident. The height of La Niña activity occurred during the 16th and 19th centuries, while the 20th century is identified as the peak period of El Niño activity. Overall, 55% of extreme El Niño event years reconstructed since A.D. 1525 occur within the 20th century. Although extreme ENSO events are seen throughout the 478-year ENSO reconstruction, approximately 43% of extreme and 28% of all protracted ENSO events reconstructed occur in the 20th century. Of particular note, the post-1940 period alone accounts for 30% of extreme ENSO years noted since A.D. 1525.

This trend towards enhanced ENSO activity is noted in the IPCC's fourth assessment report. Trenberth et al. (2007) discuss how since the 1976–1977 shift to generally above normal SSTs in the central and equatorial Pacific, there has been a tendency toward longer and stronger El Niño events (Trenberth et al. 2007). Global mean temperatures are influenced by ENSO through the large exchanges of heat between the ocean and atmosphere (Trenberth et al. 2007). For example the

1997–1998 El Niño (which produced some of the largest SST anomalies on record) occurred during 1998: one of the highest observed from the Goddard Institute for Space Studies (GISS) global mean temperatures record (Hansen et al. 2006; Trenberth et al. 2007).

Six of the Earth's warmest years recorded by the GISS record have all occurred since 1998 and the 15 warmest years in the record have all occurred since 1988 ([http://www.nasa.gov/centers/goddard/news/topstory/2008/earth\\_temp.html](http://www.nasa.gov/centers/goddard/news/topstory/2008/earth_temp.html)). Many of these warm years (e.g. 1988, 1998 and 2002) had temperatures boosted by significant El Niño events. Interestingly 2007 – the second warmest year in the GISS analysis – has occurred at a time when solar irradiance is at a minimum and the equatorial Pacific Ocean is experiencing La Niña conditions ([http://www.nasa.gov/centers/goddard/news/topstory/2008/earth\\_temp.html](http://www.nasa.gov/centers/goddard/news/topstory/2008/earth_temp.html)). This suggests that observed changes in ENSO behaviour may be more closely linked to global climate change than currently indicated by the IPCC's future climate projections (Meehl et al. 2007). If this is the case, it is possible that extremes of the hydrological cycle that produce droughts and floods during ENSO events may be enhanced under future global warming (Trenberth et al. 2007).

It is important to note, however, that reconstructions of ENSO events alone are insufficient to clearly characterise past ENSO behaviour. As one of the pioneers of ENSO modeling, Mark Cane, observed: 'if we are to trust a model to predict ENSO in the greenhouse world, it is necessary that it reproduces the changes in prior centuries' (Cane 2005:10). It is hoped that the reconstructions presented here may give us a greater appreciation of the magnitude and nature of past ENSO behaviour providing a much needed context for understanding recent observed changes required to constrain future climate change projections. Further research efforts should be directed into reconstructing ENSO variability across the entire frequency domain and reconstructing/modeling historic synoptic conditions (e.g. Fowler 2005; Cook et al. 2007). In this way, proxy reconstructions could be more readily used to constrain numerical experiments used to assess uncertainties in ENSO dynamics (e.g. response of extreme events to natural/anthropogenic forcing).

A recent comparison of a tropical SST reconstruction with two general circulation models indicates that the late 20th century is likely the warmest period in the tropics for the last 250 years, and that this recent warming can only be explained by anthropogenic forcing (Wilson et al. 2006). They note that the high frequency variability of their reconstruction is dominated by ENSO, suggesting that ENSO may operate differently in increasingly anthropogenically forced climate system. However, according to model ensemble results considered in the IPCC fourth assessment report, there is no consistent indication of how the amplitude or frequency of ENSO will operate under global warming (Meehl et al. 2007). Dynamical studies have suggested that solar, volcanic and anthropogenic radiative forcing have influenced past ENSO variability over the past millennium (Clement et al. 2001; Cane 2005; Mann et al. 2005; Cane et al. 2006). According to model results described by Cane (2005), warmer background conditions are associated with increased ENSO variability. The complexity of the atmosphere–ocean feedbacks involved in ENSO dynamics, however, leads to inconsistencies in ENSO model simulations, increasing the uncertainty of such conclusions (Collins 2005; Meehl et al. 2007). Model simulations of past ENSO variability are likely to be our best guide for projecting future patterns of temperature and rainfall caused by ENSO.

A greater understanding of ENSO is especially important for national assessments of the socio-economic risks associated with future climate change. As recognised in by the IPCC, the availability of observational data restricts the types of extremes events that can be analysed for the identification of long-term changes (Trenberth et al. 2007). Extending the current time series of ENSO events beyond the 20th century may assist natural disaster managers to revise event probabilities/return periods used for assessing risk vulnerability of biophysical and socio-economic systems to threats like water scarcity or crop failures. Improvements in quantitative predictive tools for climate risk management (e.g. rainfall forecasts, commodity price projections and long-term trends in agricultural productivity) are vital for providing early warnings of drought and crop failure risks (D'Arrigo and Wilson 2008). This is particularly relevant to policy makers and natural resource managers developing future climate change adaptation strategies. As evidence of stresses on water supply, agriculture and natural ecosystems caused by climate change strengthens (e.g. Hennessy et al. 2007), studies into how ENSO will operate in a warmer climate should be a global research priority.

**Acknowledgements** Many thanks to Penny Whetton (CSIRO) and Ian Rutherford (University of Melbourne) for the Nile Flood Record, Berlage Teak Chronology, North China Rainfall data, Erica Hendy (Lamont Doherty Earth Observatory) for Great Barrier Reef coral luminescence record, Pavla Fenwick (Lincoln University, New Zealand) for Pink Pine tree-ring data, Bruce Bauer and Connie Woodhouse (World Data Center for Paleoclimatology/National Climatic Data Center Paleoclimatology Branch) for data and advice. Particular thanks to Scott Mooney, Karl Braganza, Penny Whetton, Simon Haberle, Joshua Bassett and three anonymous reviewers for constructive comments on the manuscript. AMF was supported by the Royal Society of New Zealand Marsden Fund (Contract UOA108).

## References

- Allan R (2000) ENSO and climatic variability in the past 150 years. In: Diaz H, Markgraf V (eds) *El Niño and the Southern Oscillation: multiscale variability and global and regional impacts*. Cambridge University Press, Cambridge, pp 3–35
- Allan R, D'Arrigo R (1999) 'Persistent' ENSO sequences: how unusual was the 1990–1995 El Niño? *Holocene* 9(1):101–118
- Allan R, Lindsay J, Parker D (1996) *El Niño Southern Oscillation and climate variability*. CSIRO, Melbourne, Australia
- Baumgartner T, Michaelsen J, Thompson L, Shen G, Soutar A, Casey R (1989) *The recording of interannual climatic change by high-resolution natural systems: tree rings, coral bands, glacial ice layers and marine varves. Aspects of climate variability in the Pacific and Western Americas*. Geophysical monograph. Peterson, D. Washington. American Geophysical Union 55:1–14
- Berlage H (1931) On the relationship between thickness of tree rings of Djati and rainfall on Java. *Tectona* 24:939–953
- Bjerknes J (1966) A possible response of the atmospheric Hadley circulation to equatorial anomalies of ocean temperature. *Tellus XVIII*:820–829
- Bjerknes J (1969) Atmospheric teleconnections from the equatorial Pacific. *Mon Weather Rev* 97:163–172
- Boswijk G, Fowler A, Lorrey A, Palmer J, Ogden J (2006) Extension of the New Zealand kauri (*Agathis australis*) chronology to 1724 BC. *Holocene* 16(2):188–199
- Bouma M, Kovats R, Goubet S, Cox J, Haines A (1997) Global assessment of El Niño's disaster burden. *Lancet* 350:1435–1438
- Bradley R (1996) Are there optimum sites for global paleotemperature reconstruction? In: Jones P, Bradley R, Jouzel J (eds) *Climate variations and forcing mechanisms of the last 2000 years*. Springer-Verlag, Berlin, pp 603–624

- Braganza K, Gergis J, Power S, Risbey J, Fowler A (2008) A new Pacific basin-wide index of El Niño–Southern Oscillation, A.D.1525–1982. Centre for Australian Weather and Climate Research (CAWCR) Technical Report No. 3, CAWCR, Melbourne, Australia
- Cane M (2005) The evolution of El Niño, past and future. *Earth Planet Sci Lett* 164:1–14
- Cane M, Braconnot P, Clement A, Gildor H, Joussaume S, Kageyama M, Khodri M, Paillard D, Tett S, Zorita E (2006) Progress in paleoclimate modeling. *J Climate* 19:5031–5057
- Caviedes C (2001) El Niño in history: storming throughout the ages. University of Florida, Gainesville, USA
- Chen C, Mc Carl B, Adams R (2001) Economic implications of potential ENSO frequency and strength shifts. *Clim Change* 49:147–159
- Cleaveland M, Stahle D, Therrrell M, Villanueva-Diaz J, Burns B (2003) Tree-ring reconstructed winter precipitation and tropical teleconnections in Durango, Mexico. *Clim Change* 59:369–388
- Clement A, Cane M, Seager R (2001) An orbitally driven tropical source for abrupt climate change. *J Climate* 14(11):2369–2375
- Cobb K, Charles C, Cheng H, Edwards L (2003) El Niño/Southern Oscillation and tropical Pacific climate during the last millennium. *Nature* 424:271–276
- Cole J, Dunbar R, Mc Clanahan T, Muthiga N (2000) Tropical Pacific forcing of decadal SST variability in the Western Indian Ocean over the past two centuries. *Science* 287(5453):617–619
- Collins M (2005) El Niño or La Niña-like climate change? *Clim Dyn* 24:89–104
- Cook E, Seager R, Cane M, Stahle D (2007) North American drought: reconstructions, causes, and consequences. *Earth Sci Rev* 81(1–2):93–134
- Crowley T (2000) Causes of climate change over the past 1,000 years. *Science* 289:270–277
- D'Arrigo R, Wilson R (2008) El Niño and Indian Ocean influences on Indonesian drought: implications for forecasting rainfall and crop productivity. *Int J Climatol* 28(5):611–616. doi:10.1002/joc.1654
- D'Arrigo R, Jacoby G, Krusic P (1994) Progress in dendroclimatic studies in Indonesia. *Terrestrial, Atmospheric and Oceanographic Sciences* 5:349–363
- D'Arrigo R, Cook E, Wilson R, Allan R, Mann M (2005) On the variability of ENSO over the past six centuries. *Geophys Res Lett* 32(L03711):1–4
- D'Arrigo R, Wilson R, Palmer J, Krusic P, Curtis A, Sakulich J, Bijaksana S, Zulaikah S, Ngkoimani L, Tudhope A (2006) The reconstructed Indonesian warm pool sea surface temperatures from tree rings and corals: linkages to Asian monsoon drought and El Niño–Southern Oscillation. *Paleoceanography* 21(PA3005):PA3005/1–PA3005/13
- Dean (1993) IGBP pages/WDC-A for paleoclimatology contribution series 1993–021
- Deser C, Wallace J (1987) El Niño events and their relation to the Southern Oscillation: 1925–1986. *J Geophys Res* 92:14 189–14 196
- Diaz H, Pulwarty R (1994) An analysis of the time scales of variability in centuries-long ENSO-sensitive records in the last 1000 years. *Clim Change* 26:317–342
- Diaz H, Markgraf V (2000) El Niño and the Southern oscillation; multiscale variability and global and regional impacts. Cambridge University Press, Cambridge
- Dunbar R, Cole J (1999) Annual records of tropical systems (ARTS); recommendations for research. IGBP Science Series, Geneva, Switzerland
- Dunbar R, Wellington G, Colgan M, Glynn P (1994) Eastern Pacific sea surface temperature since 1600 AD: the d18O record of climate variability in Galapagos corals. *Paleoceanography* 9: 291–316
- Eddy J (1977) Climate and the changing sun. *Clim Change* 1:173–190
- Fedorov A, Philander G (2000) Is El Niño changing? *Science* 288:1997–2002
- Fenwick P (2003) Reconstruction of past climates using pink pine (*Halocarpus biformis*) tree-ring chronologies. Soil Plant and Ecological Sciences, Lincoln University, Christchurch, New Zealand
- Folland C, Karl T, Christy J, Clarke R, Gruza G, Jouzel J, Mann M, Oerlemans J, Salinger M, Wang S (2001) Observed climate variability and change. In: Houghton J, Ding Y, Griggs D, Noguer M, van der Linden P, Dai X, Maskell K, Johnson C (eds) Climate change 2001: the scientific basis. Contribution of working group I to the third assessment report of the intergovernmental panel on climate change. Cambridge University Press, United Kingdom and New York
- Fowler A (2005) Mean sea-level pressure composite mapping dendroclimatology: advocacy and an *Agathis australis* (kauri) case study. *Clim Res* 29:73–84
- Fowler A (2008) ENSO history recorded in *Agathis australis* (kauri) tree-rings Part B: 422 years of ENSO robustness. *Int J Climatol* 28(1):21–35

- Fowler A, Boswijk G (2003) Chronology stripping as a tool for enhancing the statistical quality of tree-ring chronologies. *Tree Ring Research* 59(2):53–62
- Fowler A, Palmer J, Salinger J, Ogden J (2000) Dendroclimatic interpretation of tree-rings in *Agathis australis* (Kauri) 2; evidence of a significant relationship with ENSO. *J R Soc N Z* 30(3):277–292
- Fowler A, Boswijk G, Ogden J (2004) Tree-ring studies on *Agathis australis* (Kauri): a synthesis of development work on late Holocene chronologies. *Tree Ring Research* 60(1):15–29
- Fowler A, Boswijk G, Gergis J, Lorrey A (2008) ENSO history recorded in *Agathis australis* (Kauri) tree-rings Part A: Kauri's potential as an ENSO proxy. *Int J Climatol* 28(1):1–20
- Gagan M, Ayliffe L, Beck J, Cole J, Druffel E, Dunbar R, Schrag D (2000) New views of tropical paleoclimates from corals. *Quat Sci Rev* 19:45–64
- Gedalof Z, Mantua N (2002) A multi-century perspective of variability in the Pacific decadal oscillation: new insights from tree rings and coral. *Geophys Res Lett* 29(24):571–573
- Gergis J (2006) Reconstructing El Niño–Southern Oscillation; evidence from tree-ring, coral, ice and documentary palaeoarchives, A.D. 1525–2002. PhD Thesis, School of Biological, Earth and Environmental Sciences, Sydney, University of New South Wales, Australia
- Gergis J, Fowler A (2005) Classification of synchronous oceanic and atmospheric El Niño–Southern Oscillation (ENSO) events for palaeoclimate reconstruction. *Int J Climatol* 25:1541–1565
- Gergis J, Fowler A (2006) How unusual was late twentieth century El Niño–Southern Oscillation (ENSO)? Assessing evidence from tree-ring, coral, ice and documentary archives, A.D. 1525–2002. *Advances in Geosciences* 6:173–179
- Gergis J, Boswijk G, Fowler A (2005a) An update of modern Northland Kauri (*Agathis australis*) tree-ring chronologies 1: Puketi State forest. New Zealand tree-ring Site Report No.19, School of Geography and Environmental Science Working Paper 29, University of Auckland, New Zealand
- Gergis J, Boswijk G, Fowler A (2005b) An update of modern Northland Kauri (*Agathis australis*) tree-ring chronologies 2: Trounson Kauri Park. New Zealand tree-ring Site Report No.20, School of Geography and Environmental Science Working Paper 30, University of Auckland, New Zealand
- Gergis J, Braganza K, Fowler A, Risbey J, Mooney S (2006) Reconstructing El Niño–Southern Oscillation (ENSO) from high-resolution palaeoarchives. *J Quat Sci* 21(7):707–722
- Goddard L, Dille M (2005) El Niño: catastrophe or opportunity. *J Climate* 18:651–665
- Goodwin I, Van Ommen T, Curran M, Mayewski P (2004) Mid latitude winter climate variability in the South Indian and Southwest Pacific regions since 1300 AD. *Clim Dyn* 22:783–794
- Greybill (1994) IGBP pages/WDC-A for paleoclimatology contribution series 1994–003
- Grissino-Mayer, Swetnam (1992) IGBP Pages/WDC-A for paleoclimatology contribution series 1992–012
- Grove R, Chappell J (2000) El Niño chronology and the history of global crises during the little ice age. In: Grove R, Chappell J (eds). *El Niño–history and crisis*. White Horse, Cambridge, pp 5–34
- Grow (2000) IGBP pages/WDC-A for paleoclimatology contribution series 2003–094
- Haberle S, Hope G, van der Kaars S (2001) Biomass burning in Indonesia and Papua New Guinea: natural and human induced fire events in the fossil record. *Palaeogeogr Palaeoclimatol* 171:259–268
- Hanley D, Bourassa M, O'Brian J, Smith S, Spade E (2003) A quantitative evaluation of ENSO indices. *J Climate* 16:1249–1258
- Hansen J, Sato M, Ruedy R, Lo K, Lea D, Medina-Elizade M (2006) Global temperature change. *Proc Natl Acad Sci U S A* 103:14288–14293
- Hassan F (1981) Historical Nile floods and their implications for climatic change. *Science* 212:1142–1145
- Hendy E, Gagan M, Alibert C, McCulloch M, Lough J, Isdale P (2002) Abrupt decrease in tropical Pacific sea surface salinity at the end of the little ice age. *Science* 295:1511–1514
- Hendy E, Gagan M, Lough J (2003) Chronological control of coral records using luminescent lines and evidence for non-stationarity ENSO teleconnections in northeastern Australia. *Holocene* 13(2):187–199
- Hennessy K, Fitzharris B, Bates B, Harvey N, Howden S, Hughes L, Salinger J, Warrick R (2007) Australia and New Zealand. In: Parry ML, Canziani OF, Palutikof JP, van der Linden PJ, Hanson CE (eds) *Climate change 2007: impacts, adaptation and vulnerability*. Contribution of working group II to the fourth assessment report of the intergovernmental panel on climate change. Cambridge University Press, Cambridge, United Kingdom and New York, NY, USA

- Holmes R, Adams R, Fritts H (1986) Users manual for program ARSTAN. Tree-ring chronologies of western North America: California, eastern Oregon and northern Great Basin. University of Arizona, Tucson, pp 50–65
- Jansen E, Overpeck J, Briffa KR, Duplessy JC, Joos F, Masson-Delmotte V, Olago D, Otto-Bliessner B, Peltier W, Rahmstorf S, Ramesh R, Raynaud D, Rind D, Solomina O, Villalba R, Zhang D (2007) Palaeoclimate. In: Solomon S, Qin D, Manning M, Chen Z, Marquis M, Averyt KB, Tignor M, Miller HL (eds) Climate change 2007: the physical science basis. Contribution of working group I to the fourth assessment report of the intergovernmental panel on climate change. Cambridge University Press, Cambridge, United Kingdom and New York, NY, USA
- Jolliffe IT (2002) Principal component analysis, 2nd edn. SpringerVerlag, New York
- Jones P, Bradley R (1992) Climate variations over the last 500 years. In: Bradley R, Jones P (eds) Climate since A.D. 1500. Routledge, London, pp 649–665
- Jones P, Mann M (2004) Climate over past millennia. *Rev Geophys* 42:1–42
- Kiladis G, Diaz H (1989) Global climatic anomalies associated with extremes in the Southern Oscillation. *J Climate* 2:1069–1090
- Kovats R, Bouma M, Hajat S, Worrall E, Haines A (2003) El Niño and health. *Lancet* 362(9394):1481–1489
- Kuhnel I, Coates L (2000) El Niño–Southern Oscillation: related probabilities of fatalities from natural perils in Australia. *Nat Hazards* 22:117–138
- Kumar A, Hoerling M (1997) Interpretation and implications of the observed inter-El Niño variability. *J Climate* 10:83–91
- Lamb S (1982) Climate, history and the modern world. Routledge, London
- Linsley B, Wellington G, Schrag D (2000) Decadal sea surface temperature variability in the subtropical South Pacific from 1726 to 1997 AD. *Science* 290:1145–1149
- Linsley B, Wellington G, Schrag D, Ren L, Salinger J, Tudhope A (2004) Geochemical evidence from corals for changes in the amplitude and spatial pattern of South Pacific interdecadal climate variability over the last 300 years. *Clim Dyn* 22:1–11
- Lough J (2004) A strategy to improve the contribution of coral data to high-resolution paleoclimatology. *Palaeogeogr Palaeoclimatol Palaeoecol* 204:115–143
- Lough J (2007) Tropical river flow and rainfall reconstructions from coral luminescence: Great Barrier Reef, Australia. *Paleoceanography* 22 (PA2218). doi:10.1029/2006PA001377
- Lyon B, Barnston A (2005) The evolution of the weak El Niño of 2004–2005. *US CLIVAR Variations* 3(2):1–4
- Mann M (2003) On past temperatures and anomalous late-20th century warmth. *Eos* 84(27):1–3
- Mann M, Bradley R, Hughes M (1998) Global-scale temperature patterns and climate forcing over the past six centuries. *Nature* 392:779–787
- Mann M, Bradley R, Hughes M (2000) Long-term variability in the El Niño/Southern Oscillation and associated teleconnections. In: Diaz H, Markgraf V (eds) El Niño and the Southern Oscillation; multiscale variability and global and regional impacts. Cambridge University Press, Cambridge, pp 327–372
- Mann M, Cane M, Zebiak S, Clement A (2005) Volcanic and solar forcing of the tropical Pacific over the past 1000 years. *J Climate* 18:447–456
- Markgraf V, Diaz H (2000) The past-ENSO record; a review. In: Markgraf V, Diaz, H (eds) El Niño and the Southern Oscillation; multiscale variability and global and regional impacts. Cambridge University Press, New York, pp 465–488
- Mc Donald J, Drysdale R, Hill D (2004) The 2002–2003 El Niño recorded in Australian cave drip waters: implications for reconstructing rainfall histories using stalagmites. *Geophys Res Lett* 31:L22202/1–L22202/4
- Meehl G, Stocker T, Collins W, Friedlingstein P, Gaye A, Gregory J, Kitoh A, Knutti R, Murphy J, Noda A, Raper S, Watterson I, Weaver A, Zhao Z (2007) Global climate projections. In: Solomon S, Qin D, Manning M, Chen Z, Marquis M, Averyt KB, Tignor M, Miller HL (eds) Climate change 2007: the physical science basis. Contribution of working group I to the fourth assessment report of the intergovernmental panel on climate change. Cambridge University Press, Cambridge, United Kingdom and New York, NY, USA
- Mendelssohn R, Bogard S, Schwing F, Palacios D (2005) Teaching old indices new tricks: a state-space analysis of El Niño related climate indices. *Geophys Res Lett* 32:L07709/1–L07709/4

- Mullan A (1995) On the linearity and stability of Southern Oscillation–climate relationships for New Zealand. *Int J Climatol* 15:1365–1386
- Murphy J, Whetton P (1989) A re-analysis of a tree-ring chronology from Java. *Proc K Ned Akad Wet (Dendrochronology) Proceedings B* 92(3):241–257
- Ortlieb L (2000) The documentary historical record of El Niño events in Peru: an update of the Quinn record (sixteenth through nineteenth centuries). In: Diaz H, Markgraf V (eds) *El Niño and the Southern Oscillation: variability, global and regional impacts*. Cambridge University Press, Cambridge, pp 207–295
- Patz J, Campbell-Lendrum D, Holloway T, Foley J (2005) Impact of regional climate change on human health. *Nature* 438:310–317
- Power S, Maylock M, Colman R, Wang X (2006) The predictability of inter-decadal changes in ENSO activity and ENSO teleconnections. *J Climate* 19:4755–4771
- Quinn W, Neal V (1992) The historical record of El Niño events. In: Bradley R, Jones P (eds) *Climate since A.D. 1500*. Routledge, London, pp 623–648
- Quinn W, Neal V, Antunez de Mayola S (1987) El Niño occurrences over the past four and a half centuries. *J Geophys Res* 92(C13):14449–14461
- Quinn T, Crowley T, Taylor F, Henin C, Joannot P, Join Y (1998) A multicentury stable isotope record from a New Caledonia coral: interannual and decadal SST variability in the southwest Pacific since 1657. *Paleoceanography* 13(4):412–426
- Rasmusson E, Carpenter T (1982) Variations in tropical sea surface temperature and surface wind fields associated with the Southern Oscillation/El Niño. *Mon Weather Rev* 110:354–384
- Rasmusson E, Carpenter T (1983) The relationship between eastern equatorial Pacific sea surface temperatures and rainfall over India and Sri Lanka. *Mon Weather Rev* 111:517–528
- Reid G (1997) Solar forcing of global climate change since the mid 17th century. *Clim Change* 37:391–405
- Rodbell D, Seltzer G, Anderson D, Abbott M, Enfield D, Newman J (1999) An ~15 000-year record of El Niño driven alluviation in southwestern Ecuador. *Science* 283:516–520
- Salinger M, Renwick J, Mullan A (2001) Interdecadal Pacific oscillation and South Pacific climate. *Int J Climatol* 21:1705–1721
- Solow A (2006) An ENSO shift revisited. *Geophys Res Lett* 33(L22602):L22602/1–L22602/3
- Stahle D, Cleaveland M (2002) IGBP pages/WDC-A for paleoclimatology contribution series 2002–004
- Stahle D, D'Arrigo R, Krusic P, Cleaveland M, Cook E, Allan R, Cole J, Dunbar R, Therrell M, Gay D, Moore M, Stokes M, Burns B, Villanueva-Diaz J, Thompson L (1998) Experimental dendroclimatic reconstruction of the Southern Oscillation. *Bull Am Meteorol Soc* 79(10):2137–2152
- Thompson L (1992) IGBP pages/WDC-A for paleoclimatology contribution series 1992–008
- Thompson L (2000) Ice core evidence for climate change in the tropics: implications for our future. *Quat Sci Rev* 19:19–35
- Thompson L, Mosley-Thompson E, Henderson K (2000) Ice-core palaeoclimate records in tropical South America since the last glacial maximum. *J Quat Sci* 15(4):377–394
- Thompson L, Mosley-Thompson E, Davis M, Henderson K, Brecher H, Zagorodnov V, Mashiotta T, Lin P, Mikhalenko V, Hardy D, Beer J (2002) Kilimanjaro ice core records: evidence of Holocene climate change in tropical Africa. *Science* 298:589–593
- Timmermann A, Oberhuber J, Bacher A, Esch M, Latif M, Roeckner E (1999) Increased El Niño frequency in a climate model forced by future greenhouse warming. *Nature* 398:694–697
- Trenberth K (1997) The definition of El Niño. *Bull Am Meteorol Soc* 78(12):2771–2777
- Trenberth K, Hoar T (1996) The 1990–1995 El Niño Southern oscillation event: longest on record. *Geophys Res Lett* 23(1):57–60
- Trenberth K, Hoar T (1997) El Niño and climate change. *Geophys Res Lett* 24(23):3057–3060
- Trenberth K, Stepaniak D (2001) Indices of El Niño evolution. *J Climate* 14:1697–1701
- Trenberth K, Jones P, Ambenje P, Bojariu R, Easterling D, Klein Tank A, Parker D, Rahimzadeh F, Renwick J, Rusticucci M, Soden B, Zhai P (2007) Observations: surface and atmospheric climate change. In: Solomon S, Qin D, Manning M, Chen Z, Marquiz M, Averyt K, Tignor M, Miller HL (eds) *Climate change 2007: the physical science basis. Contribution of Working Group I to the Fourth Assessment Report of the Intergovernmental Panel on Climate Change*. Cambridge University Press, Cambridge, UK and New York
- Urban F, Cole J, Overpeck J (2000) Influence of mean climate change on climate variability from a 155-year tropical Pacific coral record. *Nature* 407:989–993

- Von Storch H, Zwiers F (1999) *Statistical analysis in climate research*. Cambridge University Press, Cambridge
- Wang S, Zhao Z (1981) Droughts and floods in China, 1470–1979. In: Wigley T, Ingrassia M, Farmer G (eds) *Climate and history*. Cambridge University Press, Cambridge, pp 171–288
- Whetton P, Rutherford I (1994) Historical ENSO teleconnections in the eastern hemisphere. *Clim Change* 28:221–253
- Whetton P, Allan R, Rutherford I (1996) Historical ENSO teleconnections in the Eastern Hemisphere: comparisons with latest El Niño series of Quinn. *Clim Change* 32:103–109
- Wilson R, Tudhope A, Brohan P, Briffa K, Osborn T, Tett S (2006) Two-hundred-fifty years of reconstructed and modeled tropical temperatures. *J Geophys Res* 111(C10007):C10007/1–C10007/13
- Wolter K, Timlin M (1993) Monitoring ENSO in COADS with a seasonally adjusted principal component index. *Proceedings of the 17th climate diagnostics workshop*, Norman Oklahoma, NOAA/NMC/CAC, pp 52–57
- Zhang R, Rothstein L, Busalacchi A (1998) Origin of upper-ocean warming and El Niño change on decadal scales in the tropical Pacific Ocean. *Nature* 391:879–883
- Zhang Y, Wallace J, Battisti D (1997) ENSO-like interdecadal variability: 1900–1993. *J Climate* 10:1004–1020